Joint Communication and Electromagnetic Optimization of a Multiple-Input Multiple-Output Base Station Antenna

by

Ian B. Haya

B.Sc.E., University of New Brunswick, 2006

A THESIS SUBMITTED IN PARTIAL FULFILLMENT OF THE REQUIREMENTS FOR THE DEGREE OF

Master of Science in Engineering

In the Graduate Academic Unit of Electrical and Computer Engineering

Supervisors:	Brent R. Petersen, Ph.D., Electrical and Computer Eng.
	Bruce G. Colpitts, Ph.D., Electrical and Computer Eng.
Examining Board:	Mary E. Kaye, M.Eng., Electrical and Computer Eng., Chair
	Richard J. Tervo, Ph.D., Electrical and Computer Eng.
	Julian Meng, Ph.D., Electrical and Computer Eng.
	Weichang Du, Ph.D., Faculty of Computer Science

This thesis is accepted

Dean of Graduate Studies

THE UNIVERSITY OF NEW BRUNSWICK

September, 2008

To my Family.

Abstract

Recent work has shown that in nearly line-of-sight (LOS) Multiple-Input Multiple-Output (MIMO) wireless communication systems, spacing antennas according to the symbol wavelength rather than the carrier wavelength improves multiuser performance. MIMO systems have a heavy reliance on a multipath rich environment, which may not always be present in close range ultra wideband conditions. By adding reflector elements to the antenna structure, this multipath rich environment can be induced. The performance of the users with respect to the arrangement of antennas and reflector elements is a non-linear function that a genetic algorithm (GA) seems applicable for exploiting both symbol-wavelength spacing and multipath inducing reflector elements. A GA optimization is used to determine the optimum characteristics for antennas and reflector elements. MIMO system models with four users, and three, four, and five antennas are considered using a two-dimensional LOS channel with additive white noise. Subsequently, a GA optimization design and approach for solving this problem in three-dimensional space is presented. The addition of reflector elements to purposely increase multipath requires additional design considerations incorporating distributed processing, ray-tracing, and the determination of the channel impulse response.

Acknowledgements

I would like to thank my supervisors Brent Petersen and Bruce Colpitts for their guidance and assistance throughout my research work.

This research was funded by an Alexander Graham Bell Canada Graduate Scholarship from the Natural Sciences and Engineering Research Council, by the Atlantic Innovation Fund from the Atlantic Canada Opportunities Agency, and by Bell Aliant, our industrial partner.

Table of Contents

List of Tables

List of Figures

List of Symbols, Nomenclature or Abbreviations

2-D	Two-Dimensional
3-D	Three-Dimensional
AWGN	Additive White Gaussian Noise
BER	Bit Error Rate
CCI	Co-Channel Interference
CIR	Channel Impulse Response
CNSR	Communication Networks and Services Research
dB	DeciBels
DNA	Deoxyribonucleic acid
DSP	Digital Signal Processing
EVDO	Evolution-Data Optimized
GA	Genetic Algorithm
GOS	Grade of Service
ISI	Intersymbol Interference
LOS	Line of Sight
LMS	Least Mean Square
LRS	Linear Recursive Sequence
MAI	Multiple Access Interference

MDCE	MATLAB® Distributed Computing Engine
MIMO	Multiple-Input-Multiple-Output
MMSE	Minimum Mean Squared Error
MSE	Mean Squared Error
PN	Pseudorandom Noise
SINR	Signal-to-Interference-Plus-Noise Ratio
SNR	Signal-to-Noise Ratio
SWAP	Signalling Wavelength Antenna Placement
UWB	Ultra Wideband

Chapter 1

Introduction

Recent work in the area of wireless communications has shown that when antenna placements in a two-by-two MIMO system are on the order of a symbol wavelength, rather than the carrier wavelength, significant improvements can be made with respect to performance [1], [2]. This has given rise to the term of Signaling Wavelength Antenna Placement (SWAP) gain to describe the advantages. The premise of this finding is that when the antennas are spaced a symbol wavelength apart, the likelihood that the channels and received bits are correlated is minimal.

Much of the MIMO work to date relies heavily on assuming a randomized multipath rich environment to realize the maximum gains from spatial diversity [3], [4]. The fading characteristics are often modelled as Rayleigh distributions. However, in close range indoor situations, the LOS can often dominate the multipath components (modelled as Rician distributions), minimizing the prospective gains from MIMO techniques. It is therefore necessary to examine MIMO performance in LOS situations. By strategically arranging the antennas in the system to take advantage of the SWAP Gain, an optimal placement exists that will maximize the performance of the MIMO system in an LOS situation [5]. Also, it is proposed that by intentionally placing reflectors in xthe form of plates and/or solid shaped surfaces, in front of, behind,

and around the receiving elements to purposely introduce multipath components into an LOS situation, the spatial diversity performance gains from MIMO techniques can be improved to overcome the once-dominant LOS component. The extra multipath components introduced by the reflectors effectively scramble the communication channel between a transmitter and receiver in a fashion that increases the MIMO processing gains.

1.1 Background and Literature Review

In the research area of wireless communications, current generation systems are constantly being improved upon, with the advances becoming part of the next generation of standards. MIMO systems make use of multiple antennas to achieve spatial diversity and high performance [3], [6]. Recent work has shown that in MIMO systems, by spacing the antennas according to the symbol wavelength ([speed of light]/[symbol rate]) rather than the carrier wavelength, improvements can be made in optimizing the multiuser performance [1], [7], [8]. The premise of this finding is that when the antennas are spaced a symbol wavelength, or more, the likelihood that the bits are correlated is minimal and the array receives more information. When used in conjunction with an ultra wideband (UWB) spectrum, the communication system holds the potential of delivering high-speed data services to many users [2], [9].

1.2 Thesis Contribution

The objective of this thesis is to develop a joint communication and electromagnetic optimization of a MIMO UWB base station antenna. The premise of the research will be to implement a two-dimensional (2-D) design in an LOS situation to optimize antenna placements, and to describe a design in three-dimensions (3-D) that will make use of reflectors to increase the apparent electromagnetic and com-

munication size of the antenna, and exploit the advantages gained by using symbol-wavelength spacing. This will result in a high-performing antenna in a smaller package that is easier to implement in a practical environment.

However, determining the optimum placement of antennas and arrangement of reflectors is seen as a highly non-linear computationally difficult problem that depends on the number of antennas in the system, placement and orientation of reflectors, the radio channel bandwidth, the symbol rate, fading, and the distribution of the users in the wireless communication cell [10], [11]. It is proposed that through the use of a GA optimization, for a given placement of users in the cell, an optimum antenna and reflector placement can be achieved. GA optimization has seen success in many non-linear applications, but often the results from these optimizations need interpretation [12], [13], [14]. It is possible that the algorithm can converge to a local maxima/minima point rather than reach a global solution. The presence of these vestigial structures can prove to be a problem when attempting to gain information from the results. In such cases, it is important to evaluate the results in comparison to a known upper bound to give an indication on how well the GA optimization is performing.

Currently, the problem associated with effective MIMO UWB base station antennas is that they are large. The optimization of the MIMO UWB base station antenna is seen as a highly non-linear problem. Therefore, analytically a global optimization is difficult to achieve through traditional methods. An exhaustive trial-and-error method would be able to determine the optimal arrangement, but as the complexity of the system increases, the computational requirements for this method increase exponentially. Also, as wireless systems become ubiquitous, there exists the need to accommodate increasing data rates, but also increasing device numbers [15], [16].

1.3 Thesis Structure

The remainder of this document is broken down into seven chapters. Chapter 2 provides an overview of the basics of the techniques that are utilized. Chapter 3 describes in depth the design of the communication system used in this optimization. In Chapter 4, the specifics of the GA design are covered, while in Chapter 5, the parameters and results of the simulation are examined. Chapter 6 gives an in depth description and design of a 3-D expansion of the GA optimization utilizing reflector elements for increased multipath. Finally, Chapter 7 outlines future work in this area and conclusions are made in Chapter 8.

Chapter 2

Overview

2.1 MIMO Systems

A MIMO system makes use of multiple antennas to exploit spatial diversity. By placing the antennas some distance apart, the received signals from the same user will appear at each antenna in the system. Since the radio channel in many systems is often impaired by effects such as random noise, multipath interference, co-channel interference (CCI), and adjacent channel interference, the resulting signals at each antenna will be different in terms of the channel impulse response [11], [17]. The noise and interference can be considered to be uncorrelated, while the message signal appearing at each antenna will retain some correlation. However, in cases where the antenna placements are similar, there exists the probability that the noise and interference will be correlated [18], [19], [20].

In general, any M-by-N MIMO system configuration can be modeled as a matrix of channel impulse functions from the M^{th} user to the N^{th} antenna. Typically, a wireless communications system will rely on a large base station that handles the requests from the mobile users in the cell. An example of a mobile user placement and antenna placement configuration of a four-by-four system is shown in Figure 2.1.

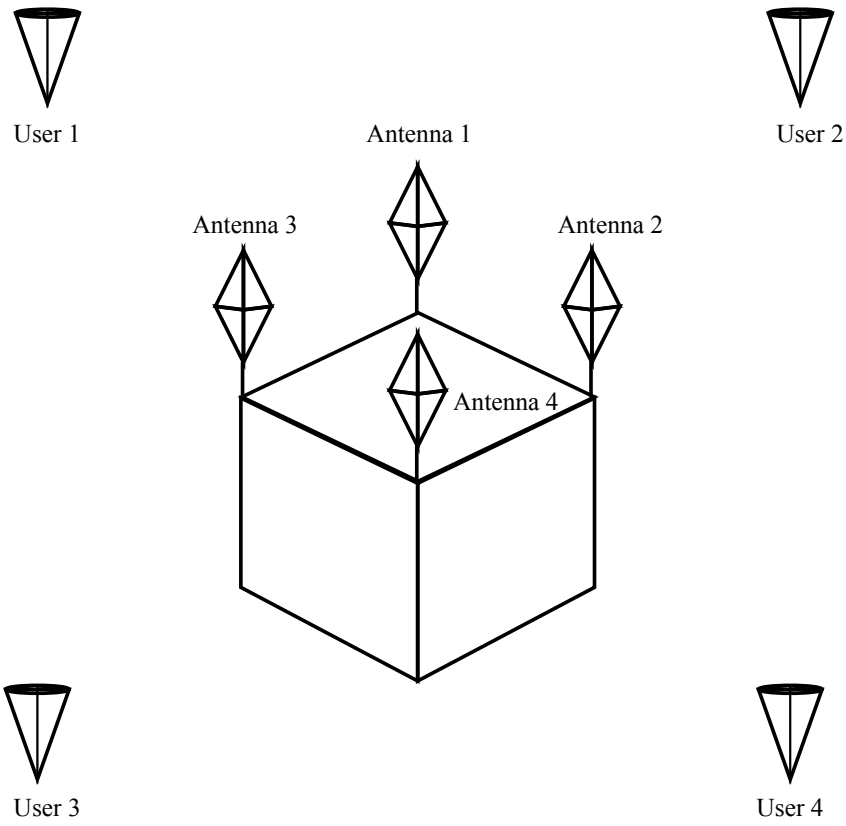

Figure 2.1: A depiction of a four-by-four arrangement for a MIMO system with mobile users placed around the antenna arrangement at the center of the cell.

2.2 Spread Spectrum Techniques

In code division multiple access (CDMA) systems, such as the Evolution-Data Optimized (EVDO) standard and direct sequence ultra wideband (DS-UWB), multiple users are multiplexed and transmitted over the same channel by using K-length pseudo random noise maximum length binary sequences, where K is the spreading factor [21], [22]. The resulting signal from a single user is thus increased in bandwidth by a factor of K. The summation of the signals from the total users produces an orthogonal signal set such that the original users signal can be de-multiplexed from the resultant signal by using the same generating code on the receive end of the channel [23], [24].

Some of the disadvantages of CDMA schemes are that they are affected more

by multiple access interference (MAI) and intersymbol interference (ISI) [15]. To allow for this, a spreading factor greater than the expected capacity is used, resulting in a greater grade of service (GOS) at the expense of more bandwidth.

2.3 Symbol Wavelength

The symbol wavelength, λ_T, is defined as

$$\lambda_T = \frac{c}{f_T}, \tag{2.1}$$

where c is the speed of light and f_T is the symbol rate. It has been shown by Yanikomeroglu et al. [1], [8] that by placing antennas on the order of a chiplength that a greater diversity gain is achieved as opposed to traditional carrier wavelength spacing. For purposes of comparison, the antenna separations in the GA optimization simulation have been normalized with respect to the symbol wavelength.

2.4 Radio Channel

The mobile radio channel is inherently noisy and cluttered with interference from other mobiles and multipath reflections. The overall performance of a wireless communication system is concerned with the multiple ways to improve the signal-to-interference-plus-noise Ratio (SINR). In 1948, Shannon demonstrated that through proper encoding in certain conditions, errors can be reduced to any desired level without sacrificing the rate of information transfer [25]. This led to the what is known as Shannon's channel capacity formula given by

$$C = B \log_2(1 + \frac{S}{N}), \tag{2.2}$$

where C is the channel capacity (bits per second), B is the transmission bandwidth (Hz), S is the signal power (W), and N is the noise power (W).

2.5 LMS Adaptive Filter

The least mean square (LMS) adaptive filter is another proven concept that has shown great performance and widespread use due to its robustness and ease of implementation [10], [26], [27]. The basic setup of an LMS adaptive filter is shown in Figure 2.2.

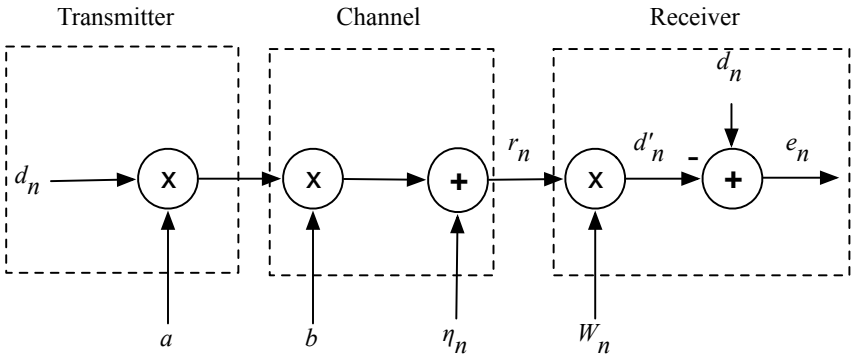

Figure 2.2: A block diagram of the described simple LMS adaptive filter.

In this arrangement, the data stream to be transmitted is given by d_n, a denotes the spreading code applied to the data, b represents the wireless channel response, η_n is the Additive White Gaussian Noise (AWGN), r_n is the signal received at the antenna, W_n is the adaptive filter coefficient, d'_n is the filtered received signal, e_n is the error associated with the filtered received signal, and n is the discrete-time index.

During training, the receiver knows d_n, as the training sequence would be programmed into the adaptive filter logic. It will then update the filter coefficient W_n according to

$$W_{n+1} = W_n + \mu e_n r_n, \tag{2.3}$$

where W_{n+1} is the updated filter coefficient, W_n is the current filter coefficient, and μ is the LMS adaptation constant, which is chosen to be small enough such that the filter will converge. If μ is chosen to be too large, the adaptation will diverge and the minimum mean square error (MMSE) will not be reached.

After the filter has finished processing the training sequence, the filter then switches from operating on the training sequence and continues to adapt from the incoming signal. Ideally at this point the adaptive filter has converged and has successfully performed the channel inversion to create a matched filter and remains at the global minimum rather than diverging off to some other local minimum. Generalizing this scalar example to vectors leads to the usual form

$$\boldsymbol{W_{n+1}} = \boldsymbol{W_n} + \mu \boldsymbol{e_n} \boldsymbol{r_n}. \tag{2.4}$$

where $\boldsymbol{W_{n+1}}$ is vector of the updated filter coefficients, $\boldsymbol{W_n}$ is a vector of the current filter coefficients, μ is the LMS adaptation constant, $\boldsymbol{e_n}$ is a vector of the error associated with the filtered receive signal, and $\boldsymbol{r_n}$ is a vector of the signals received at the antenna.

2.6 Genetic Algorithms

GA optimization borrows on the ideas of evolution found in the everyday biology of living organisms. First discussed in Charles Darwin's Origin of Species [28], the concept is that every living organism that exists today is a result of a process of evolution over the many generations that the population has existed for over great lengths of time. Within every cell of an organism, a genetic blueprint is contained within a chemical substance called deoxyribonucleic acid (DNA). This chemical substance is in a double-helical structure and contains continuous base pairs of the nucleotides adenine (A), thymine (T), guanine (T) and cytosine (C). The

sequencing of these nucleotides provides the basic genetic code that is capable of completely reproducing the organism in which the DNA is contained [12], [13]. Thus, the term DNA becomes synonymous with the minimum number of describing features that is required to fully recreate an individual or organism.

Translating this to science and engineering problems, a set of possible solutions becomes the population of living organisms. This population is then evaluated to determine their fitness to performing the desired goal defined in the problem. Such as in nature, the individuals are then subjected to a survival of the fittest evaluation, where only a portion of the top performing individuals are retained for the next generation. These top performing individuals are also chosen to be the parents for the succeeding population. These parents then generate offspring to fill the population. The offspring are generated in primarily two mechanisms, through crossover and mutation.

One of the advantages of GAs is that they are capable of operating on a problem that has a very large set of possible solutions [12], [14]. A problem with a large set of solutions may not be computationally practical to investigate through brute force methods. This leads to the advantage that GAs will often lead to solutions that would otherwise not have been reached through common numerical techniques.

Chapter 3

Communication System Design

3.1 MIMO Setup

For the genetic algorithm optimization simulation, three MIMO systems were chosen as models. This included a four-by-three, four-by-four, and four-by-five arrangements. This model configuration was chosen since it would be complex enough to exhibit characteristics of the non-linearities of the problem without being overly computationally complex. In terms of the channel impulse functions, the channel impulse response (CIR), between the users and the base stations, the channel impulse function matrix for the four-by-four system is given by

$$\mathbf{h}(t) = \begin{pmatrix} h_{11}(t) & h_{12}(t) & h_{13}(t) & h_{14}(t) \\ h_{21}(t) & h_{22}(t) & h_{23}(t) & h_{24}(t) \\ h_{31}(t) & h_{32}(t) & h_{33}(t) & h_{34}(t) \\ h_{41}(t) & h_{42}(t) & h_{43}(t) & h_{44}(t) \end{pmatrix}, \tag{3.1}$$

which has the corresponding Fourier transform

$$\mathbf{H}(f) = \begin{pmatrix} H_{11}(f) & H_{12}(f) & H_{13}(f) & H_{14}(f) \\ H_{21}(f) & H_{22}(f) & H_{23}(f) & H_{24}(f) \\ H_{31}(f) & H_{32}(f) & H_{33}(f) & H_{34}(f) \\ H_{41}(f) & H_{42}(f) & H_{43}(f) & H_{44}(f) \end{pmatrix}. \tag{3.2}$$

Variations of these can be used to model the four-by-three and four-by-five systems.

3.2 Signal Generation

For the purpose of the genetic algorithm optimization, a bandwidth spreading factor of $K = 8$ was chosen, where the highest low-pass frequency is $K/2T$, where T is the symbol period. This was chosen as a compromise between giving the coded signals enough of a spread to be recovered after noise was added to the channel, and the computational complexity associated with increasing the bandwidth of the transmitted signals. The spread spectrum spreading codes were generated randomly with complex values and unit energy.

3.3 Radio Channel Modelling

In the described GA optimization, the radio channel was modelled as being a pure LOS radio channel. In a pure LOS radio channel, the aspects of multipath interference and ground effects are ignored. The attenuation of the signal is inversely proportional to the square of the distance. This gives rise to a path loss exponent, n, of 2, and determines the received power by

$$P_r(d) = P_r(d_0) \left(\frac{d_0}{d} \right)^n, \tag{3.3}$$

where P_r is the received power (W), d_0 is a reference distance close to the base station (m), and d is the distance from the base station (m). Also, for the purpose of this simulation, the antennas were modelled as omni-directional, meaning the isotropic gain was unity.

The next point to consider is the propagation of the signals is considered to be in free space and is therefore taken as c, the speed of light. This gives rise to a time delay for the propagation from the mobile to the antennas. Using the two points of path loss and time delay, the entries of (3.2) can now be expressed as a function of the distance from mobile to the antennas to give

$$H_{ij}(f) = M_{ij}\mathrm{e}^{j2\pi f_c t_{ij}}, \tag{3.4}$$

where M_{ij} is the resulting attenuation of the signal from the i^{th} mobile to the j^{th} antenna, t_{ij} is the time delay associated with the signal from the i^{th} mobile to the j^{th} antenna, and f_c is the carrier frequency.

The sources of interference that arise in this simulation are MAI and AWGN. Complex random noise was generated and added to the received signals at each antenna. The noise variance, σ_n was chosen to give a signal-to-noise ratio (SNR) of 40 dB at each antenna.

3.4 Signal Extraction

The LMS adaptive filter was applied to each received signal at each antenna to extract the original data stream. The LMS adaptation constant, μ, was set to 2^{-5}. For the purpose of this simulation, the entire length of the data stream was considered known, and the adaptive filter was allowed to train on the whole data sequence. The LMS adaptive filter is thus able to determine the filter coefficients, $\boldsymbol{W_n}$, necessary for the mutliuser detection (Figure 3.1) for each user to antenna communication channel.

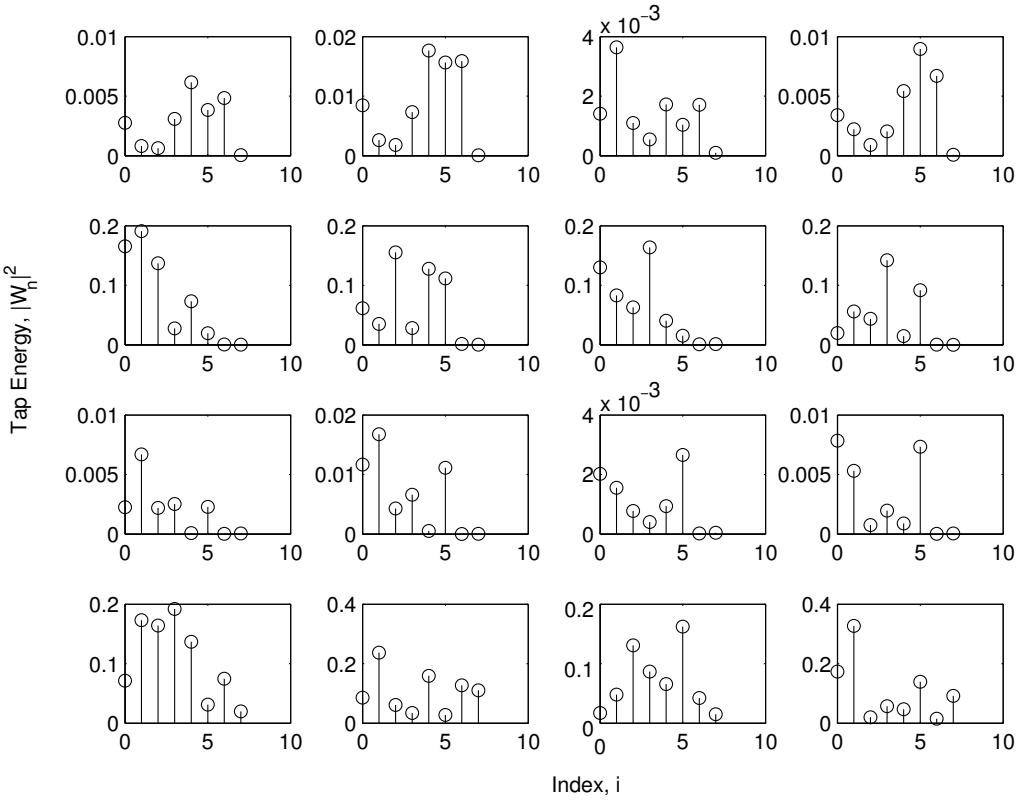

Figure 3.1: The LMS adaptive filter coefficients, $\boldsymbol{W_n}$ in terms of tap energy, versus the coefficient index, in a four-by-four MIMO system, for each user to antenna channel.

The length of the data sequence was set to be a total of 1024 bits. The adaptive filter was assumed to have converged to the global minimum and the mean squared error (MSE) was then calculated over the second half of the data stream (512 bits). The value for the MSE over the second half of the data stream was taken as the minimum mean squared error (MMSE) value for that user. The ability to detect all users in the system is imperative, thus it is necessary for all users to have converged to a near optimal MMSE value (Figure 3.2). The total performance of all the users is evaluated by averaging the MMSE results. Figure 3.2 shows that the filter has nearly converged before 400 bits have been processed. From this observation, the choice of 512 bits is a sound choice and gives reasonable results for the MMSE calculation.

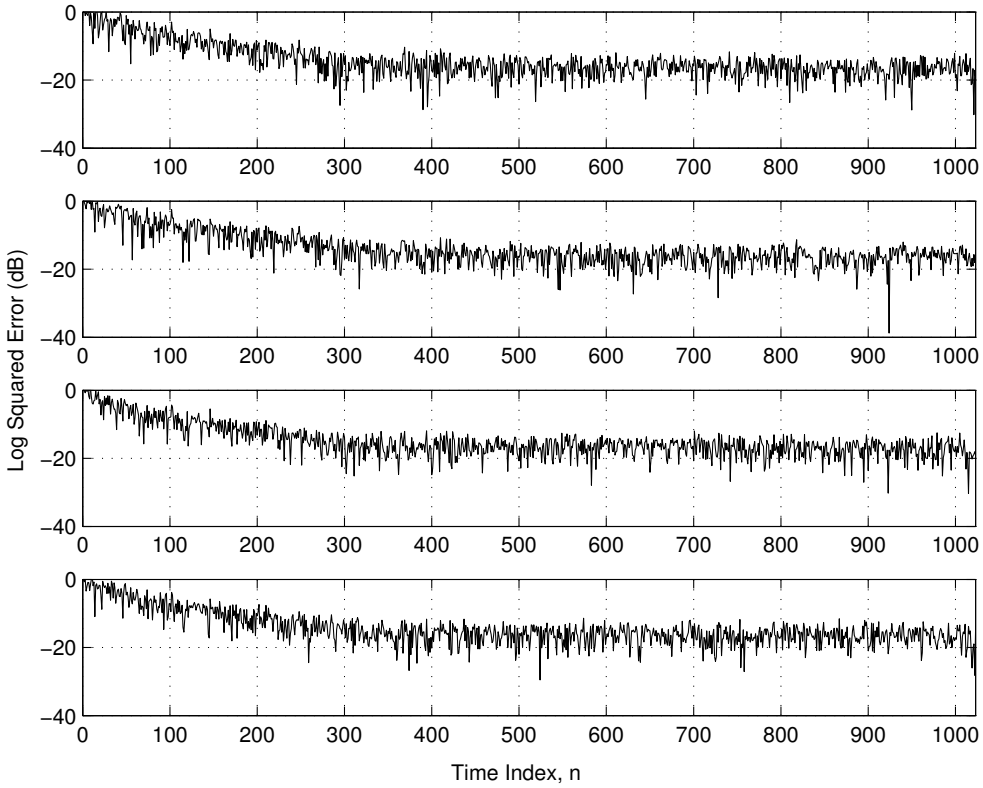

Figure 3.2: The learning curves for each user in a four-by-four MIMO system, displayed as log squared error versus time index.

Chapter 4

GA Optimization Design

4.1 Antenna DNA

In this simulation, the placement of the four antennas is chosen as the individual's DNA structure. The antenna placement is evaluated only in two dimensions, so antenna placement contains an x and y co-ordinate describing its placement within the cell. Since each individual is made up of four antenna placements, the individuals of the population can be described by

$$\mathbf{DNA_i} = \begin{bmatrix} x_1 & y_1 \\ x_2 & y_2 \\ x_3 & y_3 \\ x_4 & y_4 \end{bmatrix}. \tag{4.1}$$

This could be modified to account for N antennas by simply extending (4.1) by adding x and y co-ordinates for each additional antenna up to N. Each element is referred to as an allele of the individual, which in traditional genetics is a sequence of DNA code that is responsible for a particular characteristic in an individual. A constraint was placed on the DNA of the antennas to limit the total distance the

antennas were placed from the origin. Specifically, in the simulation, an initial constraint was placed to limit the x and y placement within the range of (-λ_T, λ_T). This was imposed to simulate some cost function associated with a given antenna placement structure. The total distance also gives a method to quantify an unstable mutation.

4.2 Fitness

For each generation of individuals that was created, it was necessary to evaluate the performance of the individuals according to a fitness function, how well the individuals were capable of achieving the specified goal. In a wireless communications system, the goal is ultimately to deliver the information reliably and efficiently. The two most common metrics that measure a systems performance in a wireless communications channel are bit error rate (BER) and the MMSE described in Section 3.4 [29]. For each individual of the antenna placement population, four MMSE values were determined, one for each user in the population. To obtain a single score for each individual in the population, the fitness function, ϕ, was given by

$$\phi = \frac{1}{\frac{1}{N}\sum_{i=0}^{N} \text{MMSE}_i}, \tag{4.2}$$

where N is the number of users.

Upon calculating ϕ, the population can then be ranked according to the resulting scores. Since a small MMSE is desired, the best scoring individuals will have a large value for ϕ. Using this choice for the fitness function, poor performing arrangements will be eliminated and the remaining arrangements will exhibit the best performance.

4.3 Generating Populations

In order to evolve, the next generation of individuals needs to inherit the properties of the top performing individuals from the previous generation and attempt to improve upon them. The portion of top performers retained for the succeeding generation was set at 10%. These top performers were chosen as the parents to generate the next population through the techniques of crossover and mutation.

4.3.1 Crossover

To generate a new individual based on the genetic technique of crossover, two parents are randomly chosen from the top performing population. A binary crossover vector is randomly generated having equal length of the DNA code. The new individual is created by using a combination of the alleles found on in the DNA codes of the two parents. In this case, on the loci (location of allele, or DNA code index) where the crossover vector is a 0, the offspring will inherit the attribute found at the same site as parent 1.

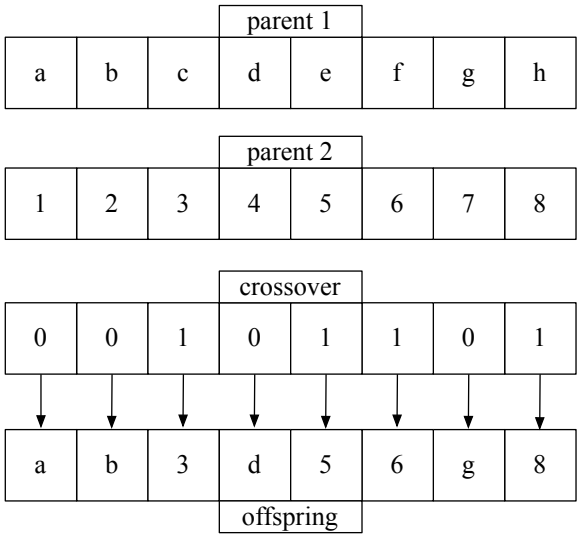

Figure 4.1: A depiction of the crossover process in which a new offspring is created by inheriting attributes from two selected elite parents.

4.3.2 Mutation

The second method by which new individuals are created is through the process of mutation. This method involves adding random perturbations to the genetic code to create new individuals that result from a morphing of the parent. In nature, this process is invoked to increase the available genetic content in a population. The mathematical equivalent to this is to give the population the ability to evolve towards a global optimization rather than remain at some local minima. Often, it is quite possible as well for individuals to be created with similar performance, but vastly different characteristics.

To generate a new individual via mutation, first, an individual is randomly selected from the top performer population to be mutated. A mutation vector of the same length as the DNA code is then generated by randomly selecting a perturbation from a zero-mean normal distribution. This perturbation vector is then added to the selected parent to create a new individual that is a resultant of the morphed values.

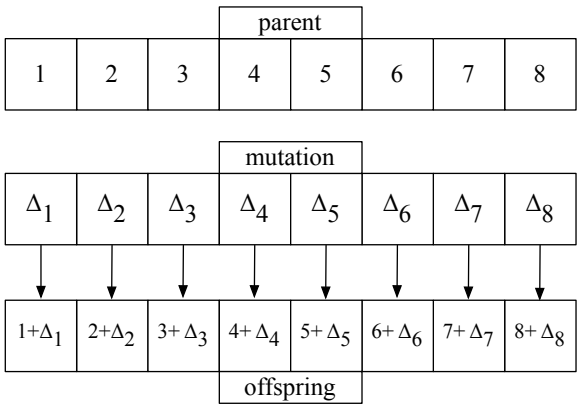

Figure 4.2: A depiction of the mutation process in which a new offspring is created by adding perturbations to the attributes of a randomly selected elite individual.

The standard deviation of the mutation vector, σ_m, was given a starting value, σ_{m_0}, and chosen as $0.1\lambda_T$, where λ_T is the symbol wavelength. Another characteristic of population genetics is that often when a population is young, it is necessary for

the mutations to be large and abundant. As the population evolves, it becomes more specialized and large mutations often appear to provide no further advantages. Also, the value of σ_m will determine the variance associated with a population. In order to meet some predefined convergence criteria, it is then necessary for the σ_m to decrease as the population becomes more specialized. This gives rise to a degradation factor, α, to determine the value of σ_m for the next population. The calculation of the σ_m is therefore give by

$$\sigma_m(\gamma) \; = \; \sigma_{m_0} \, \alpha^{\gamma - 1}, \tag{4.3}$$

where γ, is the generation index. A value for α was chosen as 0.97.

Chapter 5

Simulation

5.1 Methods

The joint optimization of the base station antenna is carried out through a computer simulation in MATLAB® run on an eight-core Mac Pro computing platform that makes use of the MATLAB® distributed computing engine (MDCE) toolbox to maximize computational throughput for the eight processing cores. Since much of the simulation involves coarse-grained parallel computations, the processor core utilization is very efficient.

5.2 Results

The simulation was coded as a MATLAB® script file. Several different user orientations were considered and the output of the optimizations was retained for each generation. For each user orientation, the population size was set to 100 individuals. The number of generations that were simulated was also 100. The selection criterion was retained as the top 10% performing individuals. A crossover ratio of 0.5 was chosen. This meant that 50% of the new individuals that were created were done so by using the crossover technique, while the remaining 50% were generated through

mutation. The same parameters were used to evaluate the four-by-three, four-by-four, and four-by-five MIMO configurations.

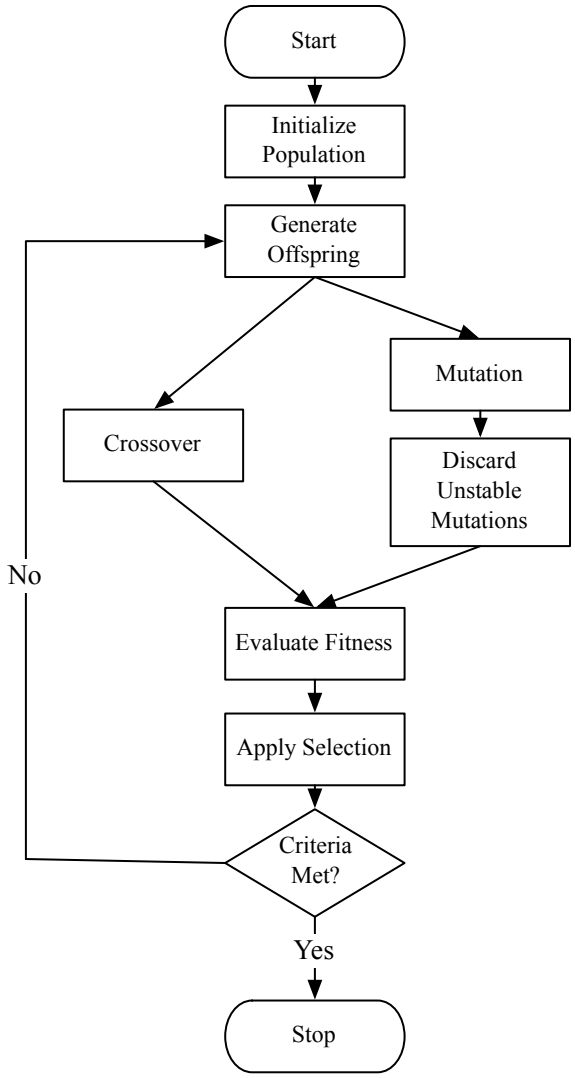

Figure 5.1: A generalized flow chart for the GA optimization process.

A second run of the simulation was repeated for the same user configurations, but this time choosing a crossover ratio of 0. This meant that the generation of new individuals was done through pure mutation. Similarly, this was also done for the four-by-three, four-by-four, and four-by-five configurations.

Figure 5.2 shows an example of one of the mobile user placements for which the simulation was run. This particular configuration shows the mobile users equally

separated around the origin of the cell, each at a radial distance of fifty λ_T.

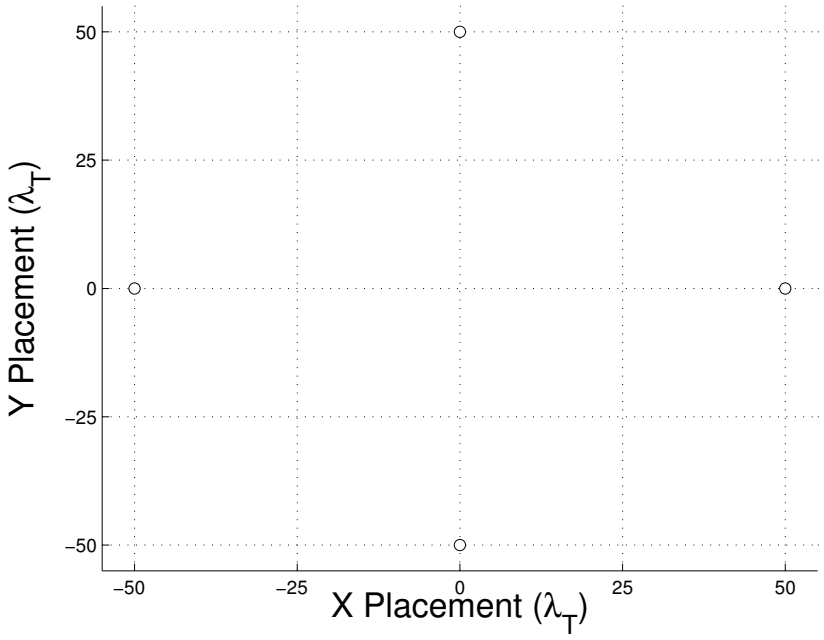

Figure 5.2: A configuration used for the placement of the mobile users in the cell.

To quantify the effectiveness of the GA optimization, the total variance of the antenna placements was evaluated using

$$\mathrm{Var}_\gamma = \sum_{k=1}^{n} \mathrm{Var}[\boldsymbol{\Delta_k(\gamma)}], \tag{5.1}$$

where Var_γ is the total variance of the generation, γ is the generation index, n is the number of unique components in the DNA, and $\boldsymbol{\Delta_k(\gamma)}$ is a vector containing all the of the k^{th} components the DNA in the generation γ. Once this value reached steady-state, it is assumed that the optimization has converged. The number of generations was fixed at 100 for this simulation. This allowed for fine tuning of the final solution in many of the cases, since several of the cases showed a vast improvement in as little as 10 generations.

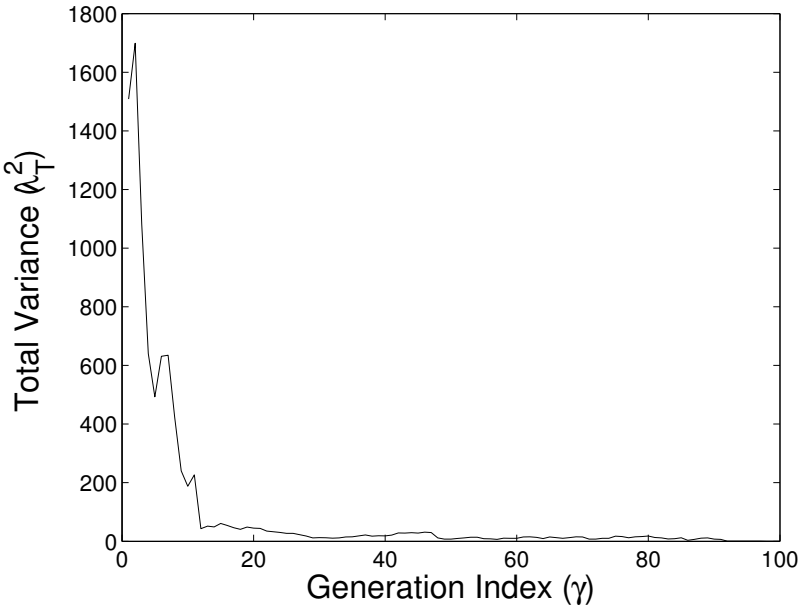

Figure 5.3: The total variance of the antenna placements versus the generation index, γ, in a four-by-three MIMO system using the mobile user placement in Figure 5.2 and a crossover ratio of 0.

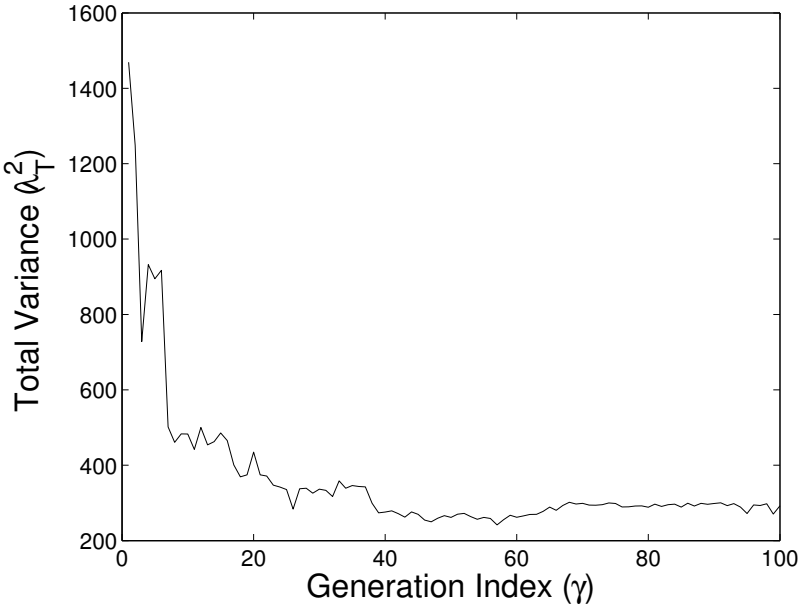

Figure 5.4: The total variance of the antenna placements versus the generation index, γ, in a four-by-three MIMO system using the mobile user placement in Figure 5.2 and a crossover ratio of 0.5.

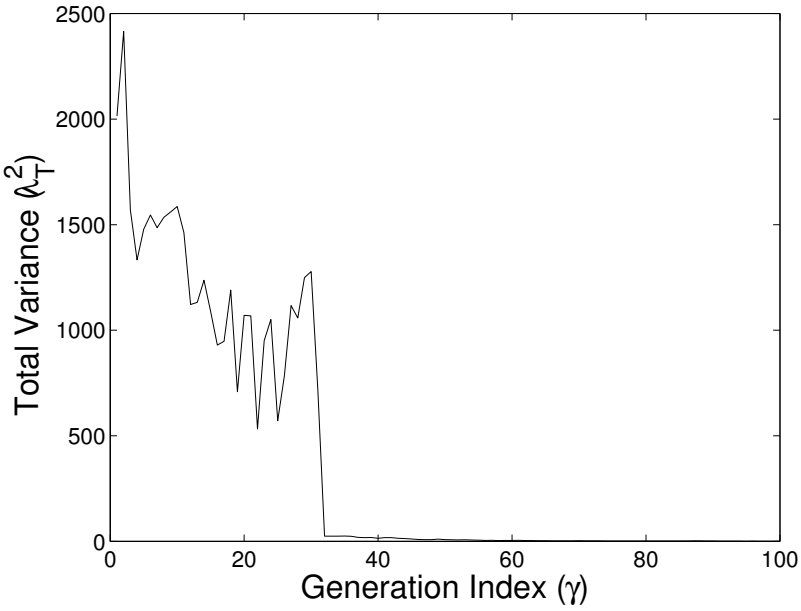

Figure 5.5: The total variance of the antenna placements versus the generation index, γ, in a four-by-four MIMO system using the mobile user placement in Figure 5.2 and a crossover ratio of 0.

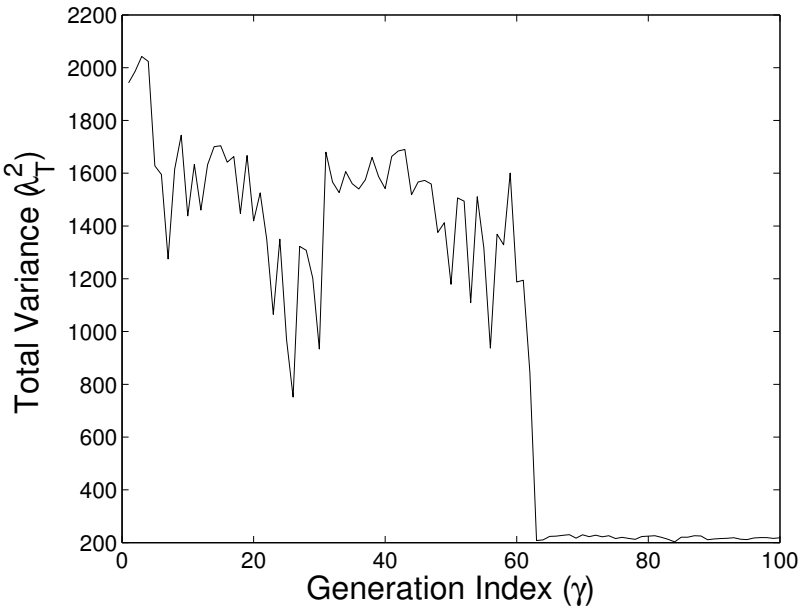

Figure 5.6: The total variance of the antenna placements versus the generation index, γ, in a four-by-four MIMO system using the mobile user placement in Figure 5.2 and a crossover ratio of 0.5.

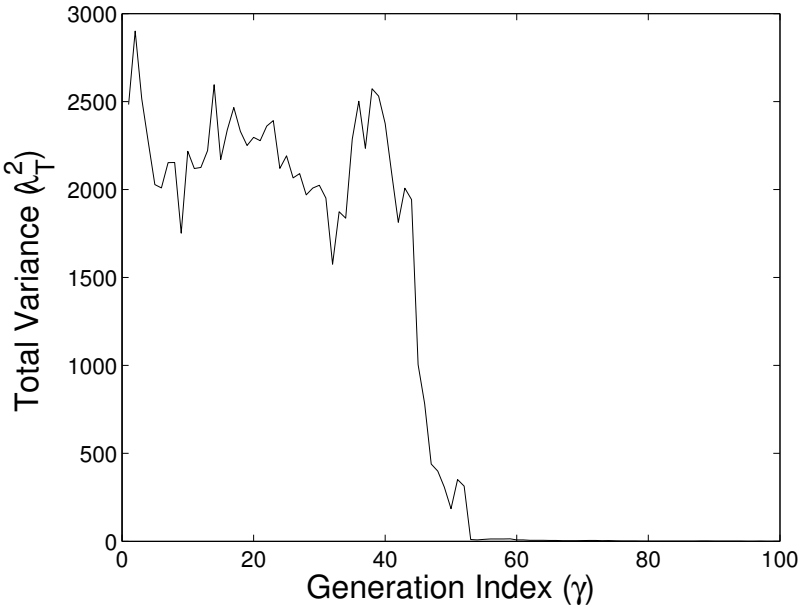

Figure 5.7: The total variance of the antenna placements versus the generation index, γ, in a four-by-five MIMO system using the mobile user placement in Figure 5.2 and a crossover ratio of 0.

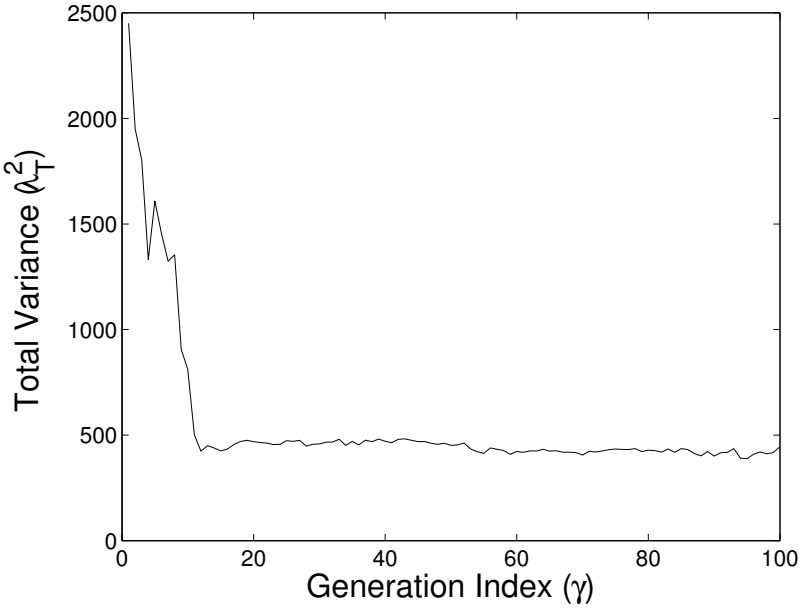

Figure 5.8: The total variance of the antenna placements versus the generation index, γ, in a four-by-five MIMO system using the mobile user placement in Figure 5.2 and a crossover ratio of 0.5.

Using a crossover ratio of 0.5, the results from the four-by-three system using the user arrangement in Figure 5.2, the antenna placement moved towards an isosceles right-angled triangle (Figure 5.9). The lengths of the equal sides of the triangle are on the order of the symbol wavelength.

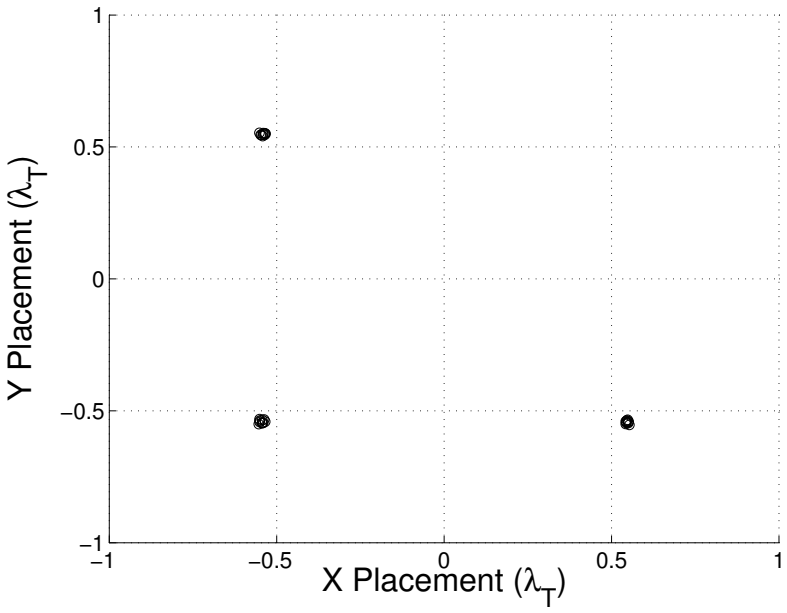

Figure 5.9: Antenna placements in a four-by-three system for the top 10% using the mobile user placement in Figure 5.2 and a crossover ratio of 0.5 after 100 generations.

Figures 5.10-5.21 show how the GA progresses during the optimization through successive generations. For the purpose of illustration, these figures show the placement of all the antennas rather than the top 10% performing individuals. Many regions for antenna placement are eliminated within the first five to ten generations. This shows the rapid beginning of the optimization within the first few generations, but also illustrates the need for further successive generations for fine tuning.

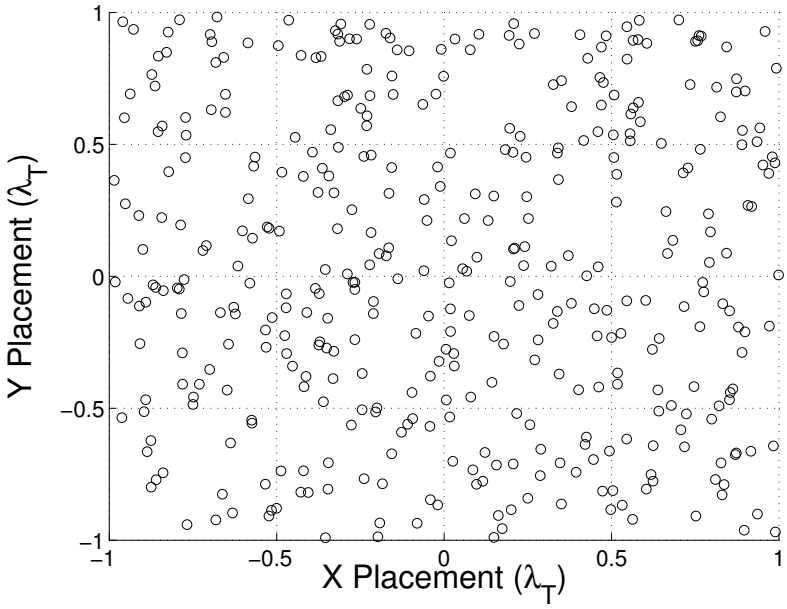

Figure 5.10: All antenna placements in a four-by-four system using the mobile user placement in Figure 5.2 and a crossover ratio of 0.5 after 1 generation.

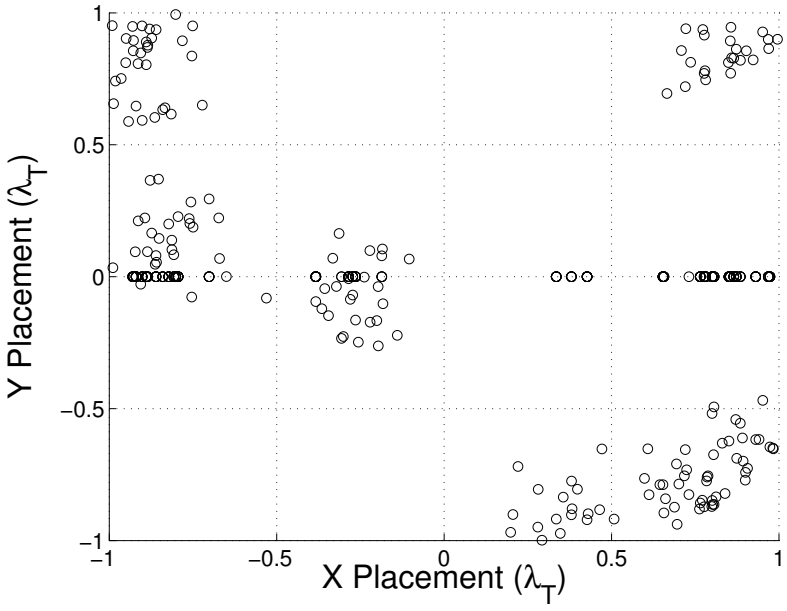

Figure 5.11: All antenna placements in a four-by-four system using the mobile user placement in Figure 5.2 and a crossover ratio of 0.5 after 5 generations.

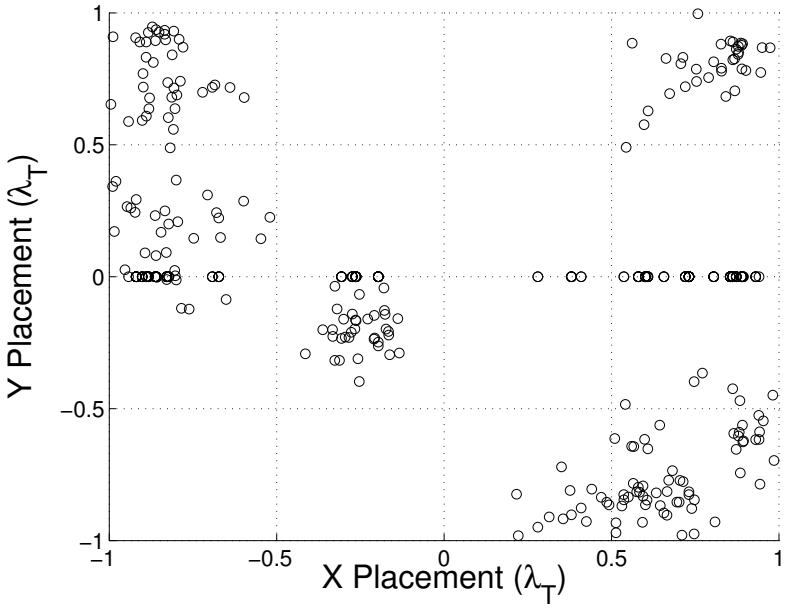

Figure 5.12: All antenna placements in a four-by-four system using the mobile user placement in Figure 5.2 and a crossover ratio of 0.5 after 10 generations.

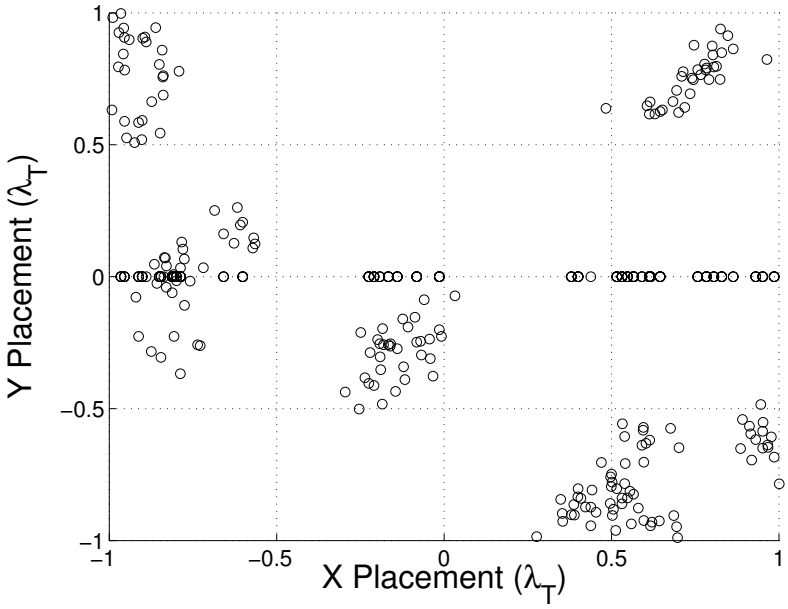

Figure 5.13: All antenna placements in a four-by-four system using the mobile user placement in Figure 5.2 and a crossover ratio of 0.5 after 20 generations.

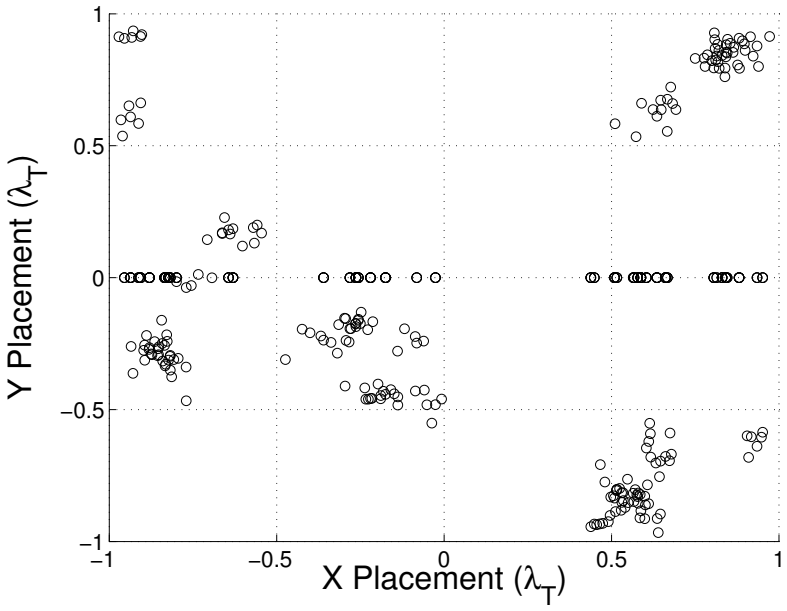

Figure 5.14: All antenna placements in a four-by-four system using the mobile user placement in Figure 5.2 and a crossover ratio of 0.5 after 30 generations.

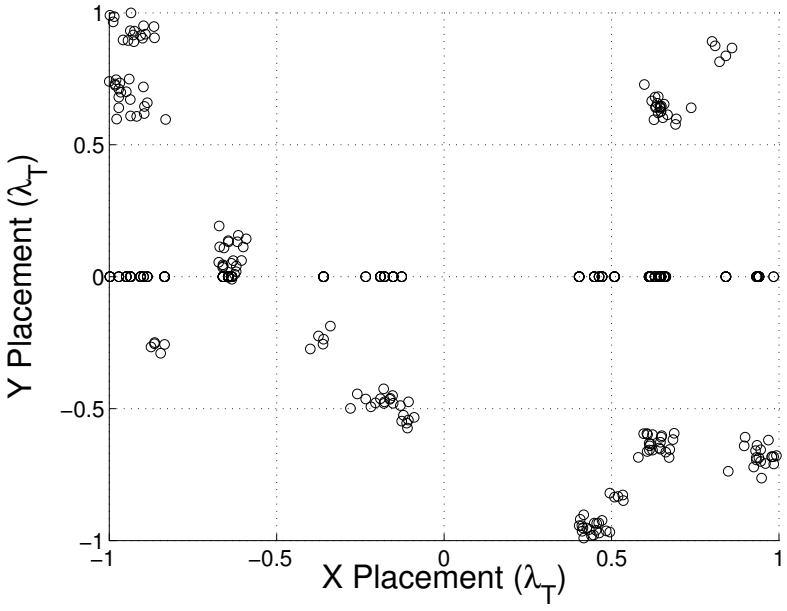

Figure 5.15: All antenna placements in a four-by-four system using the mobile user placement in Figure 5.2 and a crossover ratio of 0.5 after 40 generations.

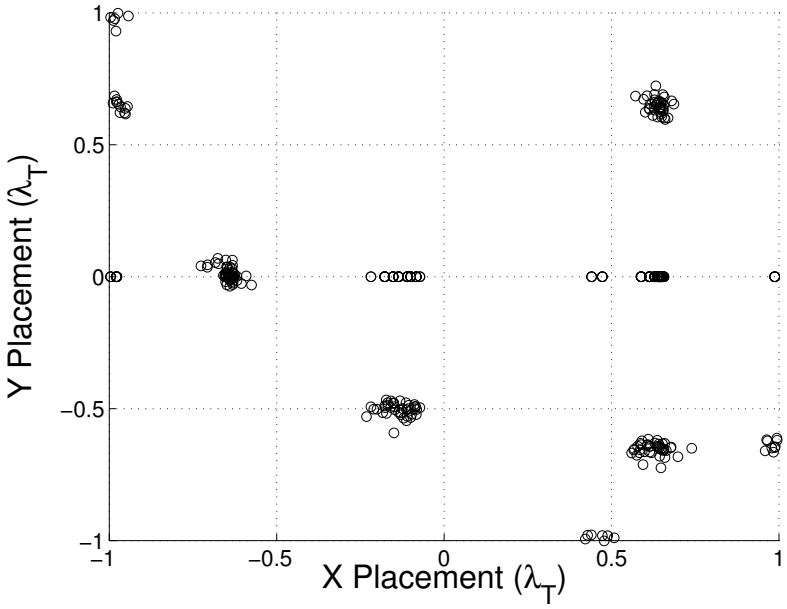

Figure 5.16: All antenna placements in a four-by-four system using the mobile user placement in Figure 5.2 and a crossover ratio of 0.5 after 50 generations.

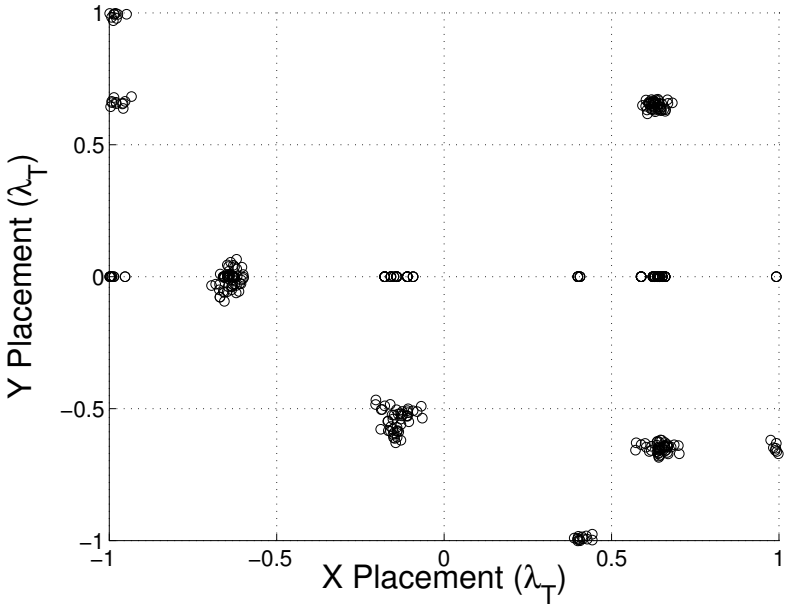

Figure 5.17: All antenna placements in a four-by-four system using the mobile user placement in Figure 5.2 and a crossover ratio of 0.5 after 60 generations.

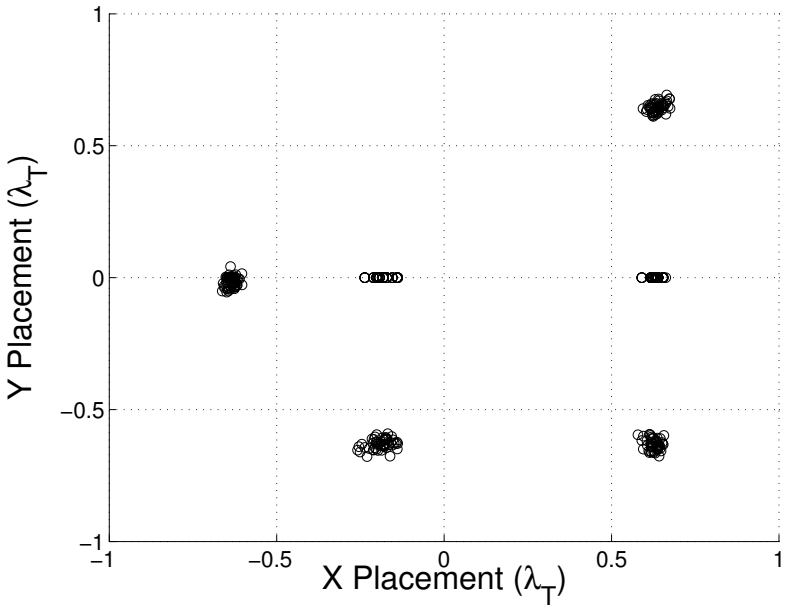

Figure 5.18: All antenna placements in a four-by-four system using the mobile user placement in Figure 5.2 and a crossover ratio of 0.5 after 70 generations.

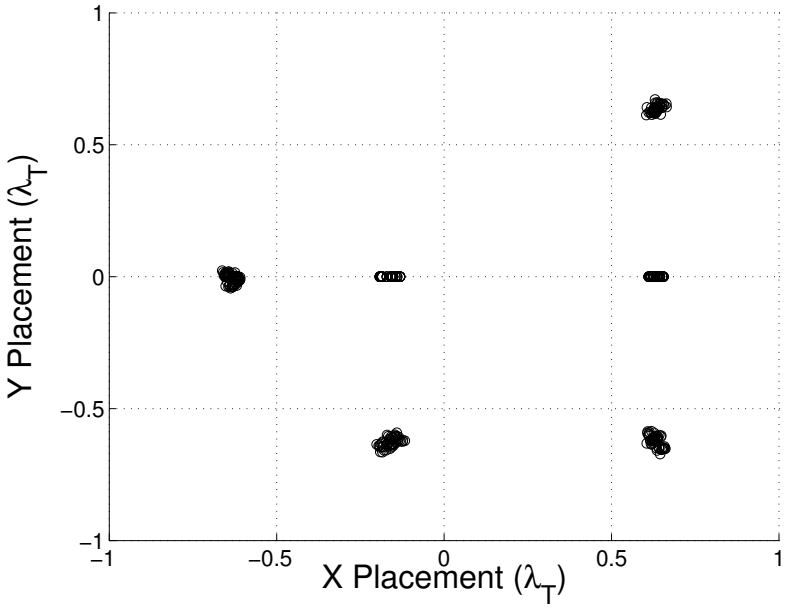

Figure 5.19: All antenna placements in a four-by-four system using the mobile user placement in Figure 5.2 and a crossover ratio of 0.5 after 80 generations.

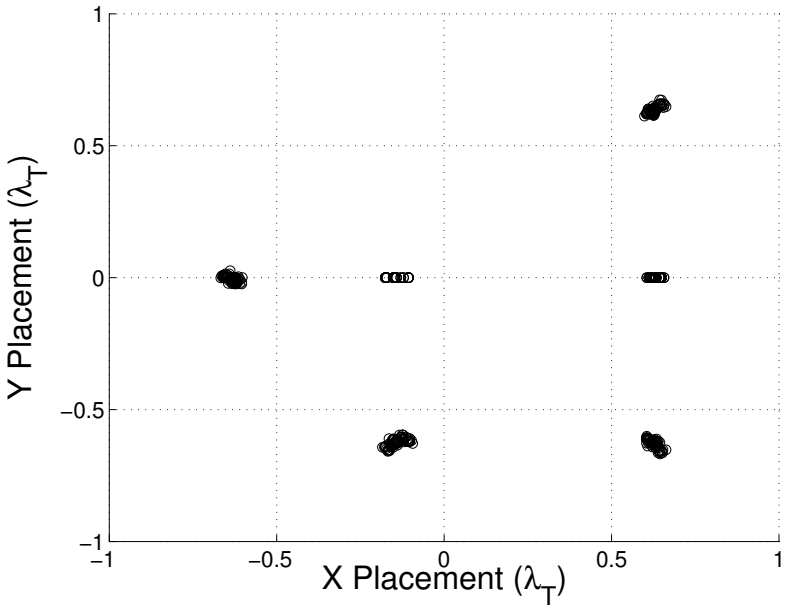

Figure 5.20: All antenna placements in a four-by-four system using the mobile user placement in Figure 5.2 and a crossover ratio of 0.5 after 90 generations.

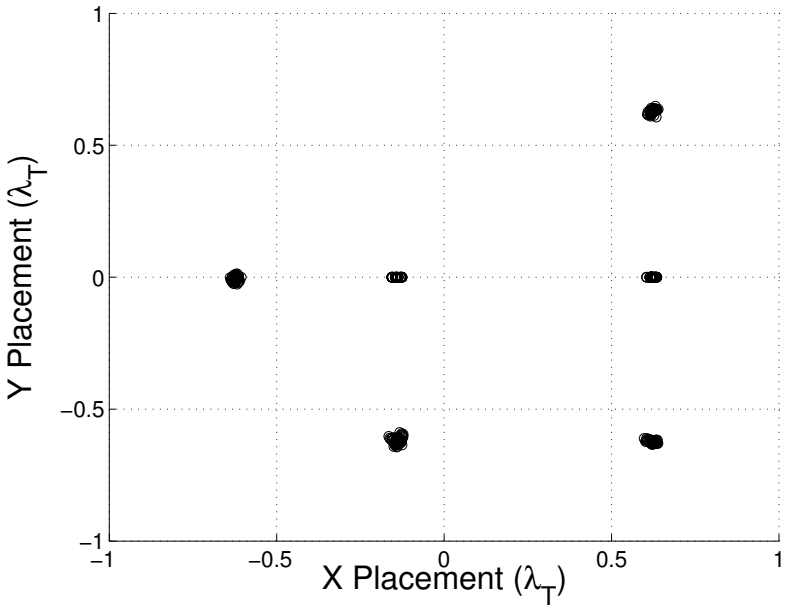

Figure 5.21: All antenna placements in a four-by-four system using the mobile user placement in Figure 5.2 and a crossover ratio of 0.5 after 100 generations.

For the initial simulation run of the four-by-four system, using a crossover ratio of 0.5, the GA tended towards an arrangement in which at least two antennas are separated by λ_T as seen by the mobile users and asymmetry (Figure 5.22). The GA is thus robust enough to encapsulate the concept of the pathological cases presented in [7] which shows symmetrical cases are to be avoided in order to benefit from spatial mutliplexing.

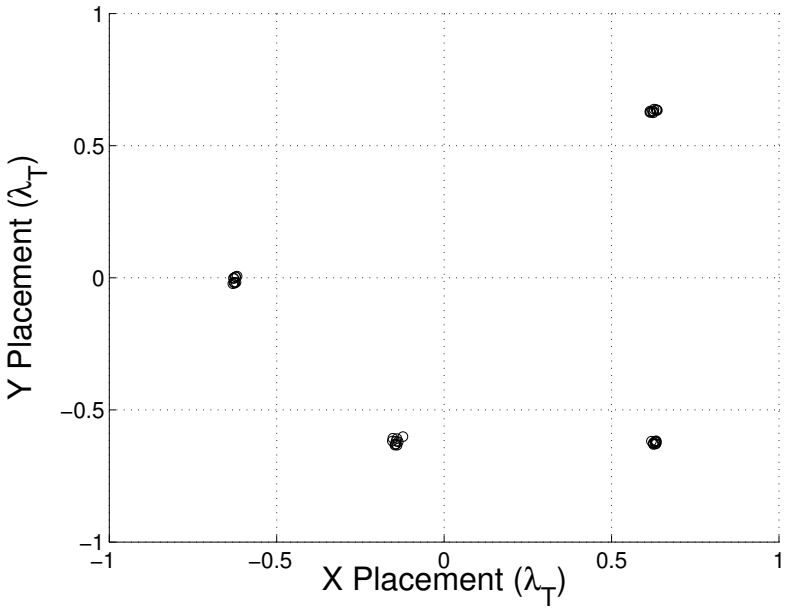

Figure 5.22: Antenna placements in a four-by-four system for the top 10% using the mobile user placement in Figure 5.2 and a crossover ratio of 0.5 after 100 generations.

The results from the simulation for the four-by-five system using a crossover ratio of 0.5 tended towards two distinct configurations (Figure 5.23) rather than the single configurations seen in the four-by-three and four-by-four simulations. While distinct, the two configurations are closely related. The four-by-five configurations show similar characteristics to those found in the four-by-four configurations. In this case, the minimum antenna separation is close to a symbol wavelength, while the maximum antenna separation is close to two symbol wavelengths.

The simulations were then repeated for each of the three systems using pure

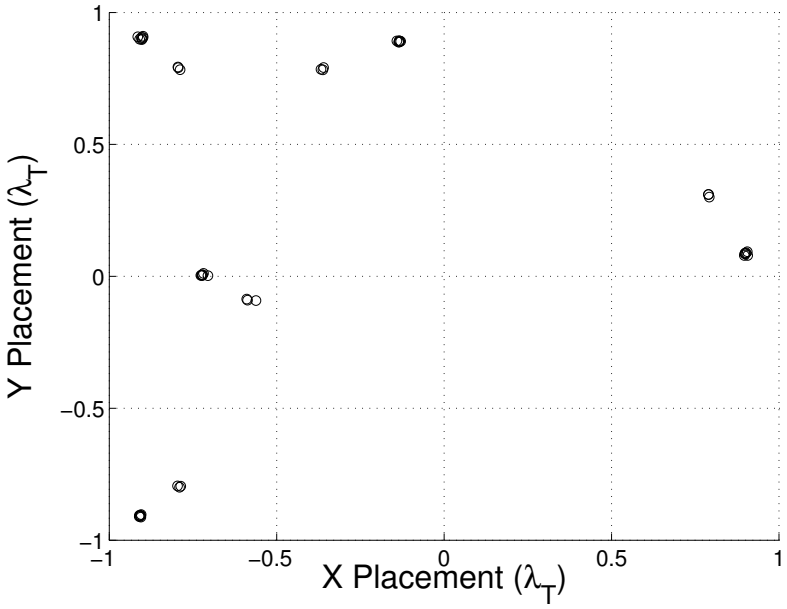

Figure 5.23: Antenna placements in a four-by-five system for the top 10% using the mobile user placement in Figure 5.2 and a crossover ratio of 0.5 after 100 generations.

mutation as the method of generating new individuals in the population. Figure 5.24 shows that the GA optimization has converged to essentially a single unique antenna arrangement. The triangular configuration has spread further than the minimum of a symbol wavelength, but the maximum antenna separation is still smaller than two symbol wavelengths.

For the next simulation run of the four-by-four system, using a crossover ratio of 0, e.g. pure mutation, the genetic algorithm tended towards a different arrangement (Figure 5.25). This arrangement also shows asymmetric qualities as well as having at least two antennas separated by λ_T as seen by the mobile users. In fact, this arrangement is a 180-degree rotation of the same antenna placement achieved through crossover, which can be considered the same result given the symmetry in the original mobile user placement. This shows that either through pure mutation, or including some degree of crossover, the same results can be achieved.

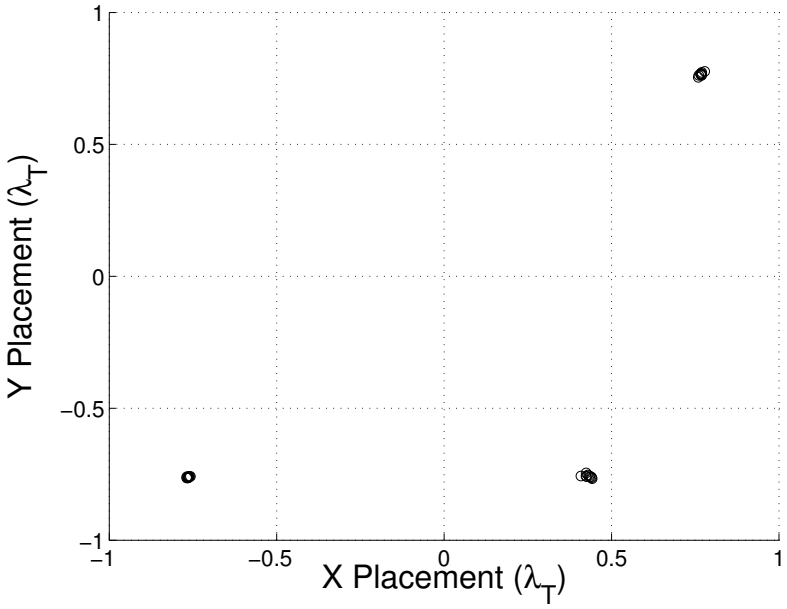

Figure 5.24: Antenna placements in a four-by-three system for the top 10% using the mobile user placement in Figure 5.2 using a crossover ratio of 0 after 100 generations.

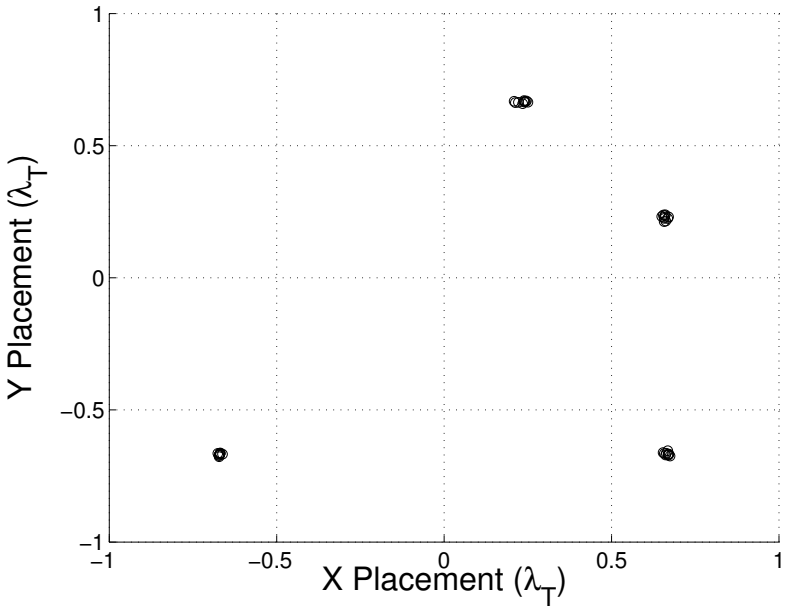

Figure 5.25: Antenna placements in a four-by-four system for the top 10% using the mobile user placement in Figure 5.2 using a crossover ratio of 0 after 100 generations.

Finally, the results of the simulation for the four-by-five system using pure mutation also converge to a single unique solution (Figure 5.26). This configuration is close to the two solutions that were found using crossover, however, it is mostly similar to the four-by-four configurations, but with a greater separation of the antennas. In this arrangement, there exists antenna separations that are closer to two symbol wavelengths in magnitude. The minimum antenna separation seen here is one instance of two antennas being closer than a symbol wavelength.

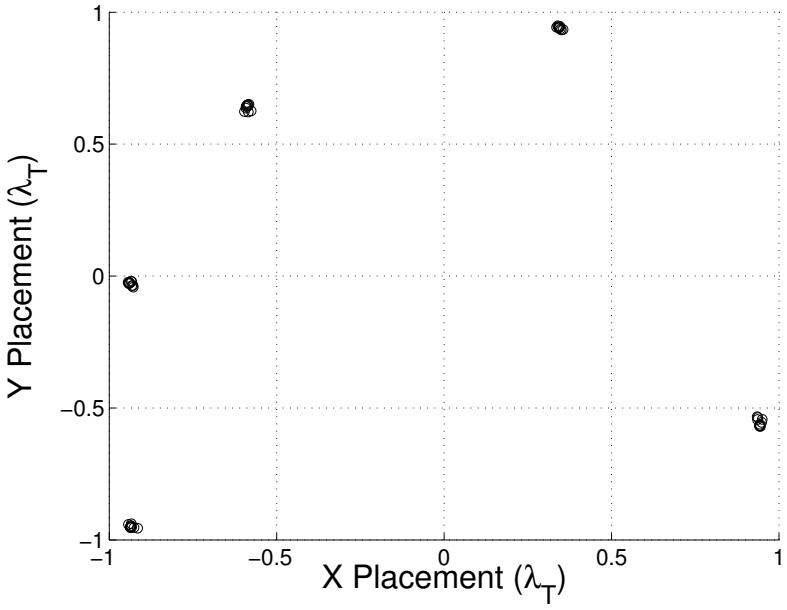

Figure 5.26: Antenna placements in a four-by-five system for the top 10% using the mobile user placement in Figure 5.2 using a crossover ratio of 0 after 100 generations.

Chapter 6

3-D Expansion

6.1 Motivation

The natural progression of the 2-D simulation work is to expand the model to 3-D space. While LOS signals alone can be simplified in the 2-D plane, it is proposed that optimal gains will be made with the addition of reflector elements to increase the multipath present in what was previously a close range LOS situation. Further increases can be made in terms of capacity and performance versus simply having the antennas in optimal positions.

6.2 Setup

An M-by-N MIMO system is considered in 3-D space, with the M users placed around the receiver structure in a known configuration. The placement and orientation of reflector and antenna elements is determined by a GA to jointly optimize the received signals based upon the electromagnetic properties of the induced communication channel and the coding scheme used in the transmitted signal.

6.3 Reflectors

The reflector elements are modelled as perfect reflectors having a reflection coefficient of unity. More realistic reflection coefficients could be incorporated in the calculations, but to simplify the simulation, a reflection coefficient of unity is used and assumed to have little effect on the overall outcome. This will maximize the gains possible from a multipath environment as well as exploit the SWAP gain.

6.3.1 Initial Placement

The placement of the reflector elements is randomly determined by the GA. They are constrained to a maximum distance from the centre point of the base station to limit the overall size of the receiver structure. Each reflector element will have a 3-D point in space corresponding to the centre point of the reflector itself. Each initial point is determined from a uniform distribution from -1 to 1 and then normalized to the maximum distance from the centre point of the base station that is chosen to constrain the GA.

The orientation of each reflector element is also randomly determined by the GA. Again, choosing from a uniform distribution from -1 to 1, three lengths are chosen for the directions along the x, y, and z axes to create a directional vector. These lengths are then normalized to create a unit directional vector that describes the plane on which the reflector will sit, centred around the origin of the reflector.

6.3.2 Size and Shape

In order to accurately simulate pure planar reflection from the reflectors, the size of the reflector elements must meet a minimum. By making the reflector elements large in comparison relative to the size of the transmitted signal's wavelengths, the effect of diffraction can be minimized. This avoids the more time consuming and

intensive process of accurately modelling diffraction.

The shape of the reflector elements are chosen as circular discs with a fixed radius. The choice of circular discs makes the most efficient use of reflector material, since this shape provides the most useable surface area with the least amount of area lost to spreading at the edges.

To simplify the calculations and simulation, all reflectors are uniform in size and shape. From a manufacturing standpoint, identical discs would be more easily machined and produced. It would be possible to allow the radius of the reflector surfaces to also be a changeable parameter in the GA. However, having the number of reflector elements as a changeable parameter, the effect of larger reflector sizes can be achieved by combining multiple smaller reflectors to create larger, more complex surfaces.

6.3.3 Growth

To facilitate the growth of the reflector elements, some consideration must be made for the addition (or subtraction) of new reflector elements. An individual in the population would begin with a certain number of reflector elements randomly placed. Through the generation of new individuals, a new parameter would be chosen for the total number of reflector elements present in a single individual.

In order to limit complexity, a maximum would be placed on the total number of reflector elements that a single individual would have. Additionally, pruning would occur that would eliminate reflector elements that did not contribute to the performance gain. This pruning would happen during the ray-tracing stage such that if it is determined that a reflector element receives no signal and does not produce a reflecting signal that is seen by the antennas, it would be eliminated from the population.

6.4 Ray-Tracing

For each individual created composing of a random arrangement of reflectors and antennas, the received signals at the antenna due to the induced multipath from the reflectors must be determined. A basic ray-tracing algorithm is implemented. Computationally, this process could be simplified by the use of a vector graphics processor. However, for simplicity, this calculation is processed generically using a general purpose central processing unit.

The CIR is determined in a similar way as in the 2-D case, consisting of the vector sum of received signals at each antenna due to propagation delay and free space path loss. However, the addition of reflectors has the added element of multipath arrivals which must be determined. The entries of the complex passband channel impulse function matrix in (3.1) become

$$h(t) = \left[\sum_{k=1}^{N} a_k \mathrm{e}^{j2\pi f_c \tau_k} \delta(t - \tau_k)\right] \star w(t), \tag{6.1}$$

where k is the multipath component index, a_k is the amplitude of the k^{th} multipath component, f_c is the carrier frequency, τ_k is the k^{th} associated propagation delay, $\star$ is the convolution operator, and $w(t)$ is an ideal low pass filter.

The total sum of multipath arrivals that are seen at the antennas is determined by ray-tracing. For each user present in an individual arrangement, directional rays are created from the users' position. Using straight lines, some granularity exists, but by setting a small enough step for degree increments, the total coverage of the ray-tracing is considered sufficient for this simulation.

From each user, based on the degree increment step specified, vectors are created over the range of $\alpha = (\text{-}\pi, \pi)$, $\gamma = (\text{-}\pi, \pi)$, and $\beta = (\text{-}\pi/2, \pi/2)$. Each vector is then used to determine the intersection point with the plane of each reflector or the region around a target antenna.

To determine whether or not the ray has intersected with a reflector plate, the intersection point with the plane of the reflector is found. To do so, the planar equation in the form of

$$ax + bx + cz + d = 0 \tag{6.2}$$

is determined, where a, b, c are the x, y, z components of the plane's normal vector,

$$\boldsymbol{n_p} = < a, b, c > . \tag{6.3}$$

Equation 6.2 can be solved for d using the values of the origin of the reflector for x, y, and z. The point of intersection lies along the ray (line) and can be found by solving for the scalar factor, s, in

$$\boldsymbol{P_{rp}} = \boldsymbol{P_{rorg}} + s\boldsymbol{d_r}, \tag{6.4}$$

where $\boldsymbol{P_{rp}}$ is the point of intersection of the ray and the reflector plate, $\boldsymbol{P_{rorg}}$ is the point of origin of the ray, s is the scaling factor, and $\boldsymbol{d_r}$ is the directional vector of the ray. The scaling factor, s, can is found by combining the line equation and the planar equation yielding

$$s = \frac{-d - \boldsymbol{P_{rorg}} \cdot \boldsymbol{n_p}}{\boldsymbol{d_r} \cdot \boldsymbol{n_p}}. \tag{6.5}$$

Substituting s back into Equation 6.4, $\boldsymbol{P_{rp}}$ can be solved for.

$\boldsymbol{P_{rp}}$ is then compared to the origin of the reflector. Based on the shape and size of the reflector, it is then determined whether or not the point of intersection from the plane and vector is within the region of the reflector. In the simple case where the reflector is a circular disc with a fixed radius, an intersection of the ray and the reflector is made if the distance from the point of intersection to the origin of the reflector is smaller than the radius. That is

$$r_p < \sqrt{(\boldsymbol{P_{rp}} - \boldsymbol{P_{porg}}) \cdot (\boldsymbol{P_{rp}} - \boldsymbol{P_{porg}})}, \tag{6.6}$$

where r_p is the radius of the reflector plate, and $\boldsymbol{P_{porg}}$ is the origin of the reflector plate, provided that the point of intersection is in the outward positive direction of the ray. This is because the general solution will provide a point of intersection along the infinite line of the ray, and the ray begins at a finite point (reflector is behind the ray). Given the assumption that the reflector surface is large compared to the incident wave, the effect of fringing and spreading is ignored and any intersection will be considered a pure reflection.

To determine whether or not the ray has intersected the region around the target antennas, the line-sphere intersection method is used. Combining the line equation,

$$\boldsymbol{P_{tint}} = \boldsymbol{P_{rorg}} + u(\boldsymbol{d_r}), \tag{6.7}$$

and the sphere equation,

$$(x - x_0)^2 + (y - y_0)^2 + (z - z_0)^2 = r_s^2, \tag{6.8}$$

yields a quadratic equation of the form

$$Au^2 + Bu + c = 0, \tag{6.9}$$

where

$$A = \boldsymbol{d_r} \cdot \boldsymbol{d_r}, \tag{6.10}$$

$$B = 2\boldsymbol{d_r} \cdot (\boldsymbol{P_{rorg}} - \boldsymbol{P_{torg}}), \tag{6.11}$$

and

$$C = (\boldsymbol{P_{rorg}} - \boldsymbol{P_{torg}}) \cdot (\boldsymbol{P_{rorg}} - \boldsymbol{P_{torg}}) - r_s^2. \tag{6.12}$$

$\boldsymbol{P_{tint}}$ is the point of intersection of the ray and the target sphere, u is a scalar, x_0, y_0, and z_0 are the respective points of origin of the sphere, $\boldsymbol{P_{torg}}$, and r_s is the radius

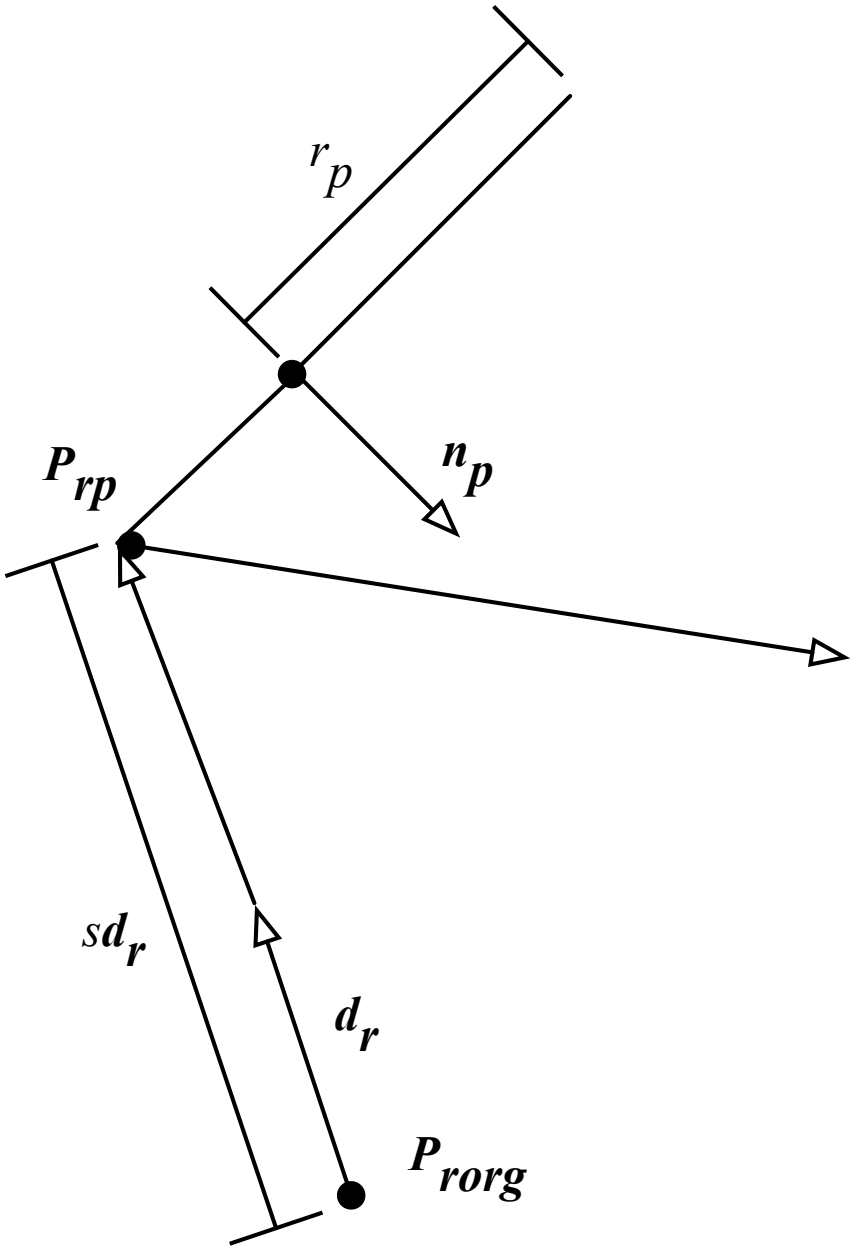

Figure 6.1: Ray-tracing to determine the intersection point, $\boldsymbol{P_{rp}}$, of a reflector plate and a ray simplified to 2-D.

of the target sphere.

Solving the quadratic equation yields two solutions, u_1 and u_2, since the line will intersect the sphere at two points, unless it is tangent to the sphere or makes no intersection at all. Substituting these values into Equation 6.7 gives the two points

of intersection. The distances, d_1 and d_2, from the origin of the ray to the points of intersection are

$$d_1 = \sqrt{\boldsymbol{P_{tint1}} \cdot \boldsymbol{P_{rorg}}}, \tag{6.13}$$

$$d_2 = \sqrt{\boldsymbol{P_{tint2}} \cdot \boldsymbol{P_{rorg}}}. \tag{6.14}$$

These solutions are considered valid if, like the reflector intersection, the signs of the vector from the ray origin to the point of intersection, that is $\boldsymbol{P_{tint}} - \boldsymbol{P_{rorg}}$, are the same as the directional vector, $\boldsymbol{d_r}$.

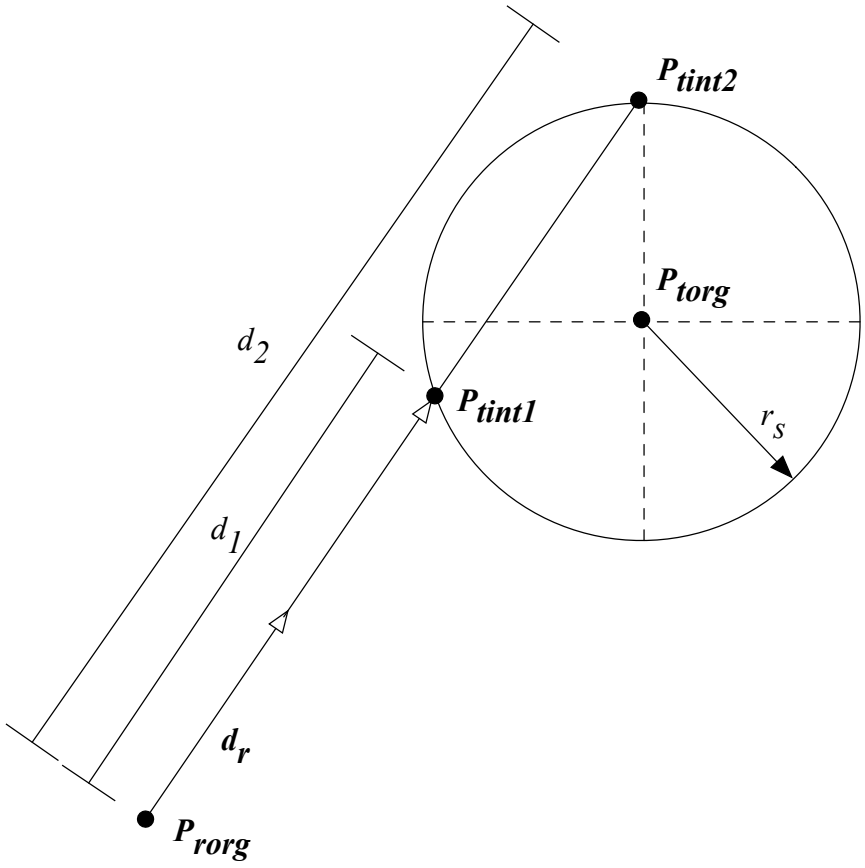

Figure 6.2: Ray-tracing to determine the intersection points, $\boldsymbol{P_{tint1}}$ and $\boldsymbol{P_{tint2}}$, of a target spherical antenna and a ray simplified to 2-D.

If an intersection is made with a target antenna, the ray is terminated if it is determined to be the the first intersection that the ray has made with either a target or other reflector. This means that the ray is terminated in this case if it has directly

made contact with a target antenna before meeting a reflector.

If a ray is determined to not make contact with either a reflector or an antenna, then it is considered to have not contributed to the received signal at the antenna, and its effects are ignored.

If a ray is found to have made an intersection with multiple reflectors, the distance between the reflector and the origin of the incident ray is determined, and the reflector that is the nearer is kept. Any intersection made with reflectors that are further away are ignored, as this would assume that the ray has been transmitted through the reflector, when in actual fact it would be in a shadowing region in which the ray would not be transmitted.

Once an intersection is made with a reflector, the point of intersection becomes the new point of origin for the reflected ray. The reflected ray is then created based upon the incident ray to the reflector. This reflected ray now becomes the new incident ray and is recursively tested for the same intersections of reflectors and antennas.

For all rays that reach the target antenna, the total path travelled becomes the summation of the vectors from the starting position of the user to each intersection points on the reflectors and end antenna. Using this total path, a multipath arrival consisting of a propagation delay and signal level based on free space path loss can be determined.

6.5 Channel Impulse Response

Once the ray-tracing has been completed, the CIR can be constructed. A single CIR for one user to one antenna will consist of the LOS path (if present) and the total summation of the multipath arrivals that have been induced by the reflectors. For the purpose of simulation, the CIR is most easily computed when described in discrete time. To limit the complexity of the calculations, the a maximum bound is

placed length of the CIR both in terms of number of samples, as well as in terms of time.

The number of samples as well as the total delay allowable for the CIR must be chosen in tandem to give an accurate representation of the effects of the multipath without sacrificing computational time. The number of samples must be large enough such that the identification of discrete paths is on the same order as path length differences based on the movement of the reflectors. The length in time of the CIR must be long enough to capture the majority of the energy from the multipath arrivals. This length can be chosen as a multiple of the symbol period to best illustrate the desired effects from symbol wavelength spacing.

6.6 GA Optimization design

The GA optimization design is built upon the 2-D design outlined in Chapter 4. The design is expanded to account for propagation in 3-D space, as well as the addition of multipath inducing reflectors.

6.6.1 Flow

Similar to the 2-D design, the basic flow of the GA optimization is as follows. The population is first seeded with individuals that are characterized by their individual DNA. The fitness function is calculated for each of these individuals to determine how well the individual is suited to meeting the specified task. In this case, the optimization is towards multiuser performance, using MMSE as the metric. Once the individuals have been scored, they are ranked and ordered. The top performing individuals are chosen to survive to the next generation, as well as serve as the parents (donors of characteristic DNA) of the next generation.

Next, the new population is generated first with the surviving elite individu-

als from the previous generation. The remaining individuals are generated using the crossover and mutation methods. As each new individual is created, those who have components that are outside the bounds (antenna or reflector too far from the origin) have those offending components removed and replaced with a newly randomly generated component. This new population then evaluates the fitness scores to once again determine the top performers. This process continues until the end criteria is met. The end criteria can be set as either a number of generations to process, or with a specific performance goal. With the latter case however, it is possible that if the specific performance goal can not be met, the simulation will loop endlessly.

6.6.2 Individual DNA

The characteristics of a single individual configuration is described by the DNA. A single individual in this population is described by the DNA for the antennas and the reflectors. The DNA parameters for the antennas is similar to that of the 2-D situation shown in (4.1), except that in this case a z-component is added to the position of the antennas to fully describe it in 3-D space. The number of antennas is fixed in this case at $N = 4$, but similarly could be modified for any N. Therefore, the antenna portion of the DNA becomes

$$\mathbf{antennas_i} = \begin{bmatrix} x_1 & y_1 & z_1 \\ x_2 & y_2 & z_2 \\ x_3 & y_3 & z_3 \\ x_4 & y_4 & z_4 \end{bmatrix}. \tag{6.15}$$

A single individual in the population also described by the reflectors surrounding the antennas. The DNA parameters that describe the reflectors are an x-y-z position in 3-D space, as well as a unit directional vector x'-y'-z' describing the orientation of the reflector plate. The shape of the reflector plate is fixed in this case to be

a circular disc of a fixed radius, which is constant for all of the reflectors. However, the total number of reflectors, N_r present in one individual configuration is variable, meaning that there is a variation in the size of the reflector portion of the DNA from Thus, the reflector portion of the DNA can be represented by

$$\mathbf{reflectors_i} = \begin{bmatrix} x_1 & y_1 & z_1 & x'_1 & y'_1 & z'_1 \\ x_2 & y_2 & z_2 & x'_2 & y'_2 & z'_2 \\ \vdots & \vdots & \vdots & \vdots & \vdots & \vdots \\ x_{N_r} & y_{N_r} & z_{N_r} & x'_{N_r} & y'_{N_r} & z'_{N_r} \end{bmatrix}. \tag{6.16}$$

In addition to the antenna and reflector DNA portions described in (6.15) and (6.16), the parameter describing the total number of reflectors, N_r, would also be contained in the DNA of the individual. Although this can easily be derived independently from the information in the reflector DNA, it is included as it is a parameter that is modified when creating new individuals using individual i as a parent.

6.6.3 Generating Populations

For the 3-D simulation, the population is initialized and generated in a similar fashion to the 2-D case as well. The position co-ordinates of the antennas are randomly generated and chosen from a uniform distribution bounded by the distance limits set from the origin of the individual structure.

For the reflectors, the number of reflectors in a given individual are randomnly generated from a uniform distribution with a limit on the maximum number of reflectors allowed. The position co-ordinates for each reflector are then chosen from a uniform distribution, as well as the lengths for the directional vector of the reflector surface. The directional vector is then normalized to unit length.

The process of creating a single individual in a population is then repeated

until the population limit is reached.

6.6.3.1 Crossover

Once the initial population has been created and evaluated, the individuals in the successive generation must be created. Mirroring the 2-D case, a new individual is created via crossover by selecting two top performing individuals from the previous generation. The new individual is generated by either inheriting information from one parent or the other from each allele, or loci of information. Since the number of reflectors is also a variable, in the case of the higher number of reflectors being chosen, the new individual will automatically inherit the reflectors from the parent to meet the desired number of reflectors.

6.6.3.2 Mutation

The second mechanisim by which new individuals are created is through mutation. This mirrors the 2-D case as well, by taking a single individual and mutating it by perturbing each parameter by a set standard deviation. Since the number of reflectors is also being perturbed in this case, the elimination of extraneous reflectors is determined randomly using a uniform distribution. In the case in which the number of reflectors needs to be increased, additional reflectors are created and added in the same way as when the population is initialized.

6.7 Distributed Processing

Given the high amount of coarse-grained parallelism in the computational requirements of implementing a GA to solve a many configurations of MIMO communication problems, great advantages can be made by incorporating distributed processing to handle these tasks. The calculations required for individuals of a pop-

ulation are not dependent on each other, therefore these lengthy linear computations can be conducted in parallel across multiple processors or nodes.

6.7.1 MDCE

One method of incorporating distributed processing techniques that was explored was through the use of the MDCE toolbox available for MATLAB®. This toolbox includes an array of utilities to implement a distributed processing solution to a set of computational tasks exhibiting parallelism. The MDCE implementation consists of the toolbox set to develop and program the work set, and the engine to run and manage the tasks. This toolbox allows not just for parallel processing across multiple workstations, but exploiting multiple processing units on a single workstation, since MATLAB® itself is currently single-threaded.

6.7.1.1 Agents

An agent in the MDCE is essentially a full instance of the MATLAB® program capable of interpreting the programs that it is assigned and carrying out the calculations. Each agent must be initialized and named such that it can be properly addressed. A single agent is the processing entity that is capable handling a task. To maximize the utilization of multiple core processors, the ideal number of agents is equal to the number of available processing cores. In a typical distributed computing hierarchy consisting of nodes in a cluster, each node (addressable physical entity) would be assigned a number of agents equal to the number of processing cores available at that node.

6.7.1.2 Job Manager

The job manager is the program responsible for assigning tasks to the agents and monitoring the exchange of information. A single job manager is required for a

single distributed problem, as it oversees the operation of all the agents in a cluster. To maximize the processor core utilization, the best performance will be achieved when a processing core is reserved for the job manager. This eliminates the downtime and queueing delays that would occur if the job manager was forced to share a processing core with an agent.

6.7.1.3 Jobs

A job in the MDCE is a task that can be assigned to an agent by the job manager. This, in its basic form is the coarse-grained independent problem that needs to be solved. The job is created by calling the desired method with the appropriate input parameters. It is then assigned an identifier and passed along to the job manager.

At this point, the job manager will take the task and assign it to the first available agent. If an agent is unavailable, the task will be queued and held onto by the job manager. Once the job has been assigned to an agent by the job manager, the job manager will wait on the completion of the operation by the agent. The agent will report back to the job manager with the results, which are then handled by the job manager.

In the implementation of the 3-D GA simulation, the calculation of the fitness function for a single individual exhibits a high amount of coarse-grained parallelism. This means that the calculation of an individuals result has no interdependence on the outcome of another individual when evaluated for the same generation. At the sub-individual level, there is also a choice within the evaluation of a single individual, ray-tracing, that may benefit from distributed process, but the overhead of the distributed setup should be evaluated as it may outweigh the gains at this level.

6.7.2 Ray-Tracing

One of the processes that may benefit from distributed processing on the sub-individual level is the ray-tracing portion. Each ray that is generated is exhaustively tracked through either multiple reflections until an intersection with a target is met, or a miss is recorded. This part of the calculation could be done in parallel by making each ray a single job.

Since the calculation of each ray is independent of the other rays from the same source, the evaluation can be carried out in parallel. However, in the simplest case in which no intersections are made, the overhead for parallel job management may be large compared to the evaluation of the ray's intersection with reflectors and targets. At low levels of complexity, i.e. a small number of reflectors and antennas, there may be no benefit seen. At higher levels of complexity, i.e. where the number of reflectors and antennas in the configuration are large, the overhead from the parallel job management becomes proportionately less.

The two main constraints to consider when deciding on the computational complexity that is tolerable is by implementing a maximum number of reflections, N_{Rmax}, to calculate as well as a ceiling on the total number of elements (reflectors and antennas), N_{Emax}. Since each ray is compared to each element, this represents a total number of N_{Rmax} evaluations for every reflection up to N_{Emax}.

6.7.3 MMSE

In the 3-D simulation expansion, the MMSE is evaluated in the same way as in the 2-D case, but with the exception that the input CIR is now more compex, having the addition of reflected multipath components. In relation to the distributed processing, the calculation of the MMSEs for an individual configuration is the at the top level of process separation. The next generation is dependent on the information gained from the MMSE calculations, and therefore the simulation cannot advance at

this point.

Therefore, as the jobs are completed (MMSE or fitness evaluated) for each individual configuration in a the present population, no further calculations are able to proceed at this point.

Since the MMSE calculation is identical to the 2-D case once the CIR has been determined, there should be no increase in the computational requirements for this section, provided the length of the CIR is the same. The approximate computational time by a single processor, discounting parallel overhead, for a generation of 100 individuals in the 2-D case was on the order of a minute, putting a complete simulation of 100 generations close to two hours. By implementing parallel processing to this portion of the GA, the potential benefit is a reduction by a factor of the number of parallel processing units, putting this computation closer to 15 min for a simulation of 100 individuals. However, the increase in number of components in the DNA may require an increase by an order of magnitude in the population size to sufficiently provide the information pool with enough unique information to reach an optimal solution.

6.7.4 Rendez-Vous

A rendez-vous point occurs at the point in which any part of the process is unable to continue without the aid of further information. As jobs are completed and the queue is emptied, there will exist some time in which there is process under-utilization as the jobs meet up at the rendez-vous point. This collective point would be seen in this situation at the points where a distributed task is being completed. If parallel tasking is used for ray-tracing, the program must wait until all rays have been traced before the CIR can be fully constructed. In the case of the MMSE fitness evaluation, all individuals in a population must complete their evaluation before they can be ranked as a group.

In general, at a rendez-vous point, the information from the parallel tasks can be collected and used to proceed with the next portion of the evaluation. Due to the nature of some problems, they are required, but proper problem separation must be used to limit the performance lost during the under-utilization stage.

Chapter 7

Future Work

Future work of this project would include verication of the findings conducted by implementation in hardware of the antenna/reflector configurations that are determined from the GA optimization. Measurements would then be carried out to determine if the simulation was able to accurately predict the multipath arrivals, and therefore if the calculated radio channels were reasonable to use in the simulation to determine the optimal antenna/reflector arrangement.

A reduction of the many designs that result from the GA optimization to the key contributing elements would be necessary as well for the future development of a commercial product. Although an attempt has been made to deduce the contributing elements in this thesis, a further test of the findings would include evaluating designs created traditionally based soley on the predicted contributing elements rather than designs created by the GA itself.

Chapter 8

Conclusion

In this thesis, a method for determining the optimum MIMO performance using omni-directional antennas in an array over LOS radio channels through GA optimization was presented. The initial results showed a tendency for the positions of the antenna placements to be in an asymmetric arrangement in which at least two antennas are separated by λ_T as seen by the mobile users. The concept of asymmetric placements can be accepted in the notion that it maximizes diversity, since symmetric configurations will produce received signals with no relative phase delay, and thus increasing the difficulty of separating the signals.

One of the reinforcing concepts that was found was that in all instances, the antenna arrangements produced a configuration in which at least two antennas were separated on the order of λ_T. This agrees with the previous findings that SWAP Gain can be achieved when antenna placements use this separation. It should be also noted that the arrangements were not likely to increase the antenna separation much more than λ_T, indicating that the performance loss from the degradation in signal power due to the excess power lost affects the placement of the antennas.

Additionally, a 3-D GA optimization design was presented that incorporated reflector elements to increase the number of multipath components. Methods were de-

veloped for solving the problem of ray-tracing and channel impulse response determination. GA parameters concerning growth, pruning, size, and shape of elements were evaluated and chosen to provide meaningful bounds on the optimization. Distributed processing was explored, while methods and recommendations for implementing these concepts to a computationally intensive GA were presented.

References

[1] G. Zhu, B. R. Petersen, and B. G. Colpitts, "Signalling wavelength in an antenna array for space-time wireless over LOS channels," in *Proceedings of the 3rd Annual Communications Networks Services and Research Conference (CNSR 2005)*, vol. 1, (Halifax, NS, Canada), pp. 69–73, May 2005.

[2] V. V. N. S. Polu, B. G. Colpitts, and B. R. Petersen, "Symbol-wavelength MMSE gain in a multi-antenna UWB system," in *Proceedings of the 4th Annual Communications Networks and Services Research Conference (CNSR 2006)*, vol. 1, (Moncton, NB, Canada), pp. 95–99, May 2006.

[3] J. Yang and S. Roy, "On joint transmitter and receiver optimization for multiple-input multiple-output (MIMO) transmission systems," *IEEE Trans. Commun.*, vol. 42, pp. 3221–3231, Dec. 1994.

[4] M. A. Jensen and J. Wallace, "A review of antennas and propagation for MIMO wireless communications," *IEEE Trans. Antennas Propag.*, vol. 52, Nov. 2004.

[5] L. Liu, W. Hong, H. Wang, G. Yang, N. Zhang, H. Zhao, J. Chang, C. Yu, X. Yu, H. Tang, H. Zhu, and L. Tian, "Characterization of line-of-sight MIMO channel for fixed wireless communications," *IEEE Antennas Wireless Propag. Lett.*, vol. 6, pp. 36–39, 2007.

[6] D. Gesbert, M. Shafi, S. Da-shan, P. Smith, and A. Naguib, "From theory to practice: an overview of MIMO space-time coded wireless systems," *IEEE J. Sel. Areas Commun.*, vol. 21, pp. 281–302, Apr. 2003.

[7] G. Zhu, "On the signalling length in digital wireless communications," Master's thesis, University of New Brunswick, Fredericton, Canada, Aug. 2005.

[8] H. Yanikomeroglu and E. S. Sousa, "Antenna gain against interference in CDMA macrodiversity systems," *IEEE Trans. Commun.*, vol. 50, pp. 1356–1371, Aug. 2002.

[9] R. Kalbasi, D. D. Falconer, and A. H. Banihashemi, "Optimum space-time processors with symbol-rate sampling are bandlimited," *IEEE Trans. Signal Process.*, vol. 54, May 2006.

[10] R. Ziegler and J. Cioffi, "A comparison of least squares and gradient equalization for multipath fading in wideband digital mobile radio," in *Conf. Rec. IEEE Globecom 89*, vol. 1, pp. 102–105, Nov. 1989.

[11] B. Widrow, P. Mantey, L. Griffiths, and B. Goode, "Adaptive antenna systems," *Proc. IEEE*, vol. 55, pp. 2143–2159, Dec. 1967.

[12] D. Fogel, "Evolutionary computing," *IEEE Spectr.*, vol. 37, pp. 26–32, Feb. 2000.

[13] D. Anastassiou, "Genomic signal processing," *IEEE Signal Process. Mag.*, vol. 18, pp. 8–20, July 2001.

[14] M. Jiang and L. Hanzo, "Multiuser MIMO-OFDM for next-generation wireless systems," *Proc. IEEE*, vol. 95, pp. 1430–1469, July 2007.

[15] P. Jung and P. Alexander, "A unified approach to multiuser detectors for CDMA and their geometrical interpretations," *IEEE J. Sel. Areas Commun.*, vol. 14, pp. 1595–1601, Oct. 1996.

[16] A. Goldsmith, S. A. Jafar, N. Jindal, and S. Vishwanath, "Capacity limits of mimo channels," *IEEE J. Sel. Areas Commun.*, vol. 21, June 2003.

[17] J. H. Winters, "Optimum combining in digital mobile radio with cochannel interference," *IEEE J. Sel. Areas Commun.*, vol. 2, pp. 528–539, July 1984.

[18] S. Roy, *Space-Time Processing Techniques with Application to Broadband Wireless Systems*. PhD thesis, Department of Systems and Computer Engineering, Carleton University, Aug. 2000.

[19] C. S. Bontu, D. D. Falconer, and L. Strawczynski, "Diversity transmission and adaptive MLSE for digital cellular radio," *IEEE Trans. on Vehicular Technology*, vol. 48, pp. 1488–1502, Sep. 1999.

[20] A. Sayeed and V. Raghavan, "Maximizing MIMO capacity in sparse multipath with reconfigurable antenna arrays," *IEEE J. Sel. Topics Signal Process.*, vol. 1, pp. 156–166, June 2007.

[21] A. J. Viterbi, *CDMA: Principles of Spread Spectrum Communication*. Reading, MA, USA: Addison-Wesley Publishing Co. Inc., 1995.

[22] A. Soong and W. Krzymien, "Effect of antenna diversity on performance of reference symbol assisted interference cancellation in CDMA wireless systems," in *Conf. Rec. 1997 IEEE 6th International Conference on Universal Personal Communications (ICUPC)*, vol. 1, pp. 202–207, Oct. 1997.

[23] S. Roy and D. D. Falconer, "Multi-user decision-feedback space-time equalization and diversity reception," in *Conf. Rec. IEEE International Conference on Vehicular Technology (VTC '99)*, vol. 1, (Houston, TX, USA), pp. 494–498, May 16-19, 1999.

[24] S. Roy and D. D. Falconer, "Optimum infinite-length MMSE multi-user decision-feedback space-time processing in broadband cellular radio," *Wireless Personal Commun.*, vol. 27, pp. 1–32, Oct. 2003.

[25] T. S. Rappaport, *Wireless Communications, 2nd ed.* Upper Saddle River, New Jersey, USA: Prentice Hall PTR, 2001.

[26] G. Cherubini, E. Eleftheriou, and S. Ölçer, "Filtered multitone modulation for very high-speed digital subscriber lines," *IEEE J. Sel. Areas Commun.*, vol. 20, pp. 1016–1028, June 2002.

[27] A. M. Legnain, D. D. Falconer, and A. U. H. Sheikh, "New adaptive combined space-time receiver for multiuser interference rejection in synchronous CDMA systems," in *Conf. Rec. Canadian Conference on Electrical and Computer Engineering (CCECE)*, vol. 1, (Waterloo, ON, Canada), pp. 421–424, May 24-28, 1998.

[28] C. Darwin, *The Origin of Species.* 1859.

[29] J. H. Winters, "Upper bounds for the bit error rate of optimum combining in digital mobile radio," in *Conf. Rec. IEEE Globecom 84*, vol. 1, pp. 173–178, Nov. 1984.

Vita

Candidate's full name: Ian Bryce Haya

University attended: University of New Brunswick, B.Sc.E., 2006

Publications:

Ian B. Haya, Brent R. Petersen, Bruce G. Colpitts, "Optimum 2-D LOS MIMO performance using omni-directional antennas attained through genetic algorithms", *IEEE Proceedings of the 6th Annual Conference on Communication Networks and Services Research (CNSR 2008)*, vol. 1, pp. 331-338, Halifax, NS, 5th-8th May 2008.